Performance Analysis of Adaptive Power Saving Mechanisms in Delay Tolerant Network

BY

SANGHO LEE

A Thesis Submitted to the Faculty of Graduate Studies

The University of Manitoba

In Partial Fulfillment of the Requirements for the Degree of

MASTER OF SCIENCE

Department of Electrical and Computer Engineering

University of Manitoba

Winnipeg, Manitoba, Canada

Abstract

Delay Tolerant Network (DTN) is emerging as a solution for supporting data transfer in intermittently connected networks. In DTN, to cope with long disconnections, messages are buffered for a long period of time. Thus, according to the queue management the performance can be affected significantly. Power is also a scarce resource in DTN. Energy can be saved by putting mobile nodes into sleep during long delayed connections. In this thesis, a Medium Access Control (MAC) protocol that supports adaptive sleep scheduling of a mobile node is proposed. Based on the MAC layer operation, an adaptive power management framework is developed. The framework considers power saving and buffer management together in order to minimize power consumption while minimizing the performance degradation of buffer management for the mobile node. Variations of the performance of a traffic source node which are affected by diverse network parameters are also investigated.

Acknowledgements

First of all, I would like to express my sincere gratitude to my advisor Dr. Attahiru Sule Alfa for his continuous guidance, kind support, and great enthusiasm for my research. His inspiration and encouragement always stimulated me to pursue my studies.

I would also like to extend my thanks to other members of my advisory committee, Dr. Dimos Polyzois and Dr. Dean McNeill, for their insightful and helpful comments and suggestions on my research and report.

Much appreciation goes to the people of my research group, particularly, Mostafizur, Yunhan, and Jungwoo for their technical discussions in my research.

Special thanks go to my friends for their help and support during the time I was doing this work, particularly Rudy and Ruth Friense, Cornel and Martha Rempel, and Ken Motts and Joyce Meckbach.

I am very grateful also to my family for their constant encouragement and support. And finally, I would like to thank my wife, Jennifer for her love, support, and understanding through out my research.

Contents

List of Figures

Chapter 1

Introduction

In the past decade, there has been an extraordinary growth in wireless communications due to the advantages of providing great flexibilities in our everyday lives. The growth has been accelerated with the development of wireless network infrastructures, applications, and mobile devices. On the other hand, recent technology advancements enable new services and thus impose new requirements on system capabilities that were not taken into consideration in the development of the current 3G system design.

Not to limit the service availability in infrastructured areas, wireless networking has to be provided where infrastructure is not available. High mobility has to be fully supported for the network transparency, such as dynamically changing network addresses and device locations. Various wireless networks need to be integrated in order to provide seamless wireless services. Very high data transmission speed has to be supported in order to enable multimedia services on mobile devices. Battery power has to be extended to support enhanced portability. To meet

these new requirements and overcome the limitations and problems of current 3G systems, new architectures and capabilities are needed for the next-generation wireless systems.

Recently, many research efforts have been devoted to extending the services to challenged environments such as deep space, disaster areas, highways, sensor fields, battle fields, and rural areas. Ad hoc wireless networking is a technology that enables wireless services to be provided in these situations. This ad hoc technology allows network nodes to communicate directly to each other without any fixed infrastructure. This is a very distinguishing feature of ad hoc networks with respect to the traditional wireless networks, such as cellular networks and wireless LAN, in which nodes communicate with each other through base stations. Due to its non-infrastructure nature, ad hoc networking, including both fixed and mobile scenarios, is expected to become an important part of the future wireless network architecture.

Mobile Ad hoc Network (MANET) is a transient network formed dynamically by a collection of arbitrarily located wireless mobile nodes without the use of existing network infrastructure or centralized administration [1]. In MANET, nodes can directly communicate with each other if they enter into each other's communication range. In addition, MANET provides multihop communication inside a group of mobile nodes. However, end-to-end connectivity is not a natural property of MANET. As the nodes are mobile, the network structure changes dynamically and this may lead to undesired situations of nodes becoming disconnected from parts of the network. High nodes mobility makes hard to establish and maintain

multihop routes, resulting in low performance. The traditional store-and-forward routing protocols cannot be employed in highly disconnected ad hoc networks. In traditional MANET nodes are assumed to be deployed dense enough to provide end-to-end paths among source and destination nodes and node mobility is assumed to be low. While this approach provides a way to deliver data fast, deploying a dense network could be unnecessarily expensive or even not allowed in challenged environments. Differently from other wireless ad hoc networks, MANET has faced, until now, poor commercial deployment despite of the significant amount of research work.

Delay Tolerant Network (DTN) is emerging as a solution for supporting asynchronous data transfer in such intermittently connected networks. Applications of such networks can be found in disaster relief networks, rural networking, environmental monitoring networks, vehicular networks, and interplanetary networks [2][3][4][5]. On the other hand, there are many challenges that must be addressed before DTN is put into practice.

1.1 Motivation

As in other wireless mobile communication architectures, power is a scarce resource for many DTN architectures. The capacity of the battery determines how long the device can be used before replacing or recharging the battery. Unlike other network architectures, DTN is characterized by frequent disruptions and disconnections between nodes. However, existing routing protocols in DTN assume radio is always turned on where nodes waste energy during idle modes. Many

researches have been conducted on power saving methods in wireless networks, such as 802.16 and MANET. However, there have been limited studies addressing the mechanism of power saving in DTN. Therefore, considerable savings in energy can realized by putting mobile devices into sleep during long delayed connections and when frequent connection is not necessary.

The major issue in designing power management for DTN is that a node needs to determine when it must communicate with other nodes, so that it can sleep during the rest of the time. The effect of power saving is even more pronounced in DTN than in MANET. The main assumption in MANET is that nodes are deployed densely enough to form a connected network most of the time while a network may become partitioned for a long time in DTN.

Another important issue in DTN is queue management. In DTN, to cope with long disconnections, messages are buffered for a long period of time. However, the assumption of availability of infinite buffer is not realistic. So, in this thesis the buffer size available at each node is limited . This implies that at certain point of time buffer capacity will be reached and messages arriving after that time will be dropped. Thus, according to the queue management employed, the performance of network could be affected significantly.

Along with the important issues in DTN, there are several important parameters that greatly affect network performance. An important parameter of DTN is the so-called contact opportunity between nodes. Two nodes are said to be in contact

if they are within transmission range of one another and thus packet exchange between them is possible. The duration of a contact impacts the performance under such a networking approach. Another key factor for the performance is the inter-contact time, which is defined as the time duration between two consecutive contacts of node pairs. The number of neighbor nodes in the radio range of a node is also important since it affects the message transmission rate and connection availability in MANET as well as in DTN. These parameters, such as contact opportunity, inter-contact time, and number of neighbor nodes affect the queuing performance of nodes and mainly depend on the mobility of the nodes. The mobility of the nodes can be characterized by network parameters, such as radio transmission distance of a node, node speed, and node density in the networks.

In this thesis, an adaptive power management framework is developed that considers power saving and buffer management together in order to minimize power consumption while minimizing the performance degradation of buffer management for a mobile node. Diverse variations of the performance of DTN are also investigated, which are affected by network parameters described above.

The power consumption can be reduced by employing proper methods for discovering contacts. In DTN structure, a periodically broadcasted beacon signal is used for a mobile node to find the contact of source node or destination node. Therefore, energy can be saved by putting mobile nodes into sleep during the time nodes are not in the contact range of traffic sources or destinations. The adaptive power saving mechanism is based on sleep scheduling of mobile nodes in Medium Access Control (MAC) layer that determines when a mobile node should switch

between active and inactive states. The choice of sleep interval also affects the performance of the protocol since tradeoffs exist between power consumption and contact discovering probability, and the effects are resulted in the performance of buffer management.

1.2 Thesis Contributions

In the following, we describe the main contributions of this thesis:

- A MAC protocol that can support adaptive sleep scheduling of a mobile node is proposed. The MAC protocol describes when a mobile node starts to sleep or when it is awake; how long the node keeps sleeping; and, how the node communicates with the source or the destination node. The mechanism includes three different sleep interval scheduling schemes with two different channel access scheduling schemes. Based on the MAC layer operation, an adaptive power management framework is developed. The framework considers power saving and buffer management together in order to minimize power consumption while minimizing the performance degradation of buffer management for the mobile node.

- The proposed sleep interval scheduling schemes are analyzed to investigate the relation between power saving and queueing performance of a mobile node. In the analysis, three-dimensional discrete time semi-Markov chain is considered for the mobile node's location, buffer level of the mobile node, and the stage of mobile node's operating mode. Through the model, the impact of sleep scheduling and traffic rate on power saving, packet loss,

delay, and throughput is investigated.

- The performance of a traffic source node for the proposed MAC protocol is analyzed by an embedded Markov chain. Two-dimensional discrete time semi-Markov chain is considered for the number of mobile nodes in the contact area of source node and buffer level of the source node. Through the numerical example, the impact of MAC parameters, node mobility, and traffic rate on packet loss, delay, and throughput is investigated. In addition, admissible buffer size of source node and admissible mobility parameters of mobile nodes that satisfy QoS requirements are determined. From the results of the analysis of mobile node and source node, the end-to-end performance of DTN is also investigated.

- Finally, in order to reflect more realistic network environment in our performance analysis, the details of DTN parameters are investigated. The node arrival rate, node's contact time, and inter-contact time from node's mobility parameters, such as radio transmission distance of a node, node speed, and node density in the networks are derived. Then, for tractable use in analysis the parameters are expressed as Phase Type (PH) model. The performance of a mobile node using this general model is analyzed and compared with the results using exponential expression of contact and inter-contact time.

1.3 Organization of the Thesis

The rest of the thesis is organized as follows: We summarize related works in chapter 2. In Chapter 3, we describe proposed power saving and MAC scheme

with performance analysis of a mobile node. In Chapter 4, we analyze the queueing performance of a source node for the proposed MAC scheme. We state derivation of the node arrival rate, contact time, and inter-contact time in chapter 5. In this chapter, we also evaluate the performance analysis of a mobile node using general PH parameter model. Finally, we summarize the results of this thesis and discusses the future works in chapter 6.

Chapter 2

Literature Review

2.1 Examples of DTN Scenarios

Burgess et al. [2] introduced a vehicular network made up of 30 buses equipped with 802.11b wireless interfaces and GPS devices. The objective of the network is to provide real DTN test bed for experimental and research studies. The buses move on regular trajectories on campuses and surrounding areas. When two buses pass near each other, they transfer data to each other.

Juang et al. [3] designed ZebraNet as a wireless sensor networking architecture to support wildlife tracking for biology research. In ZebraNet, the network consists of sensor collars that are attached to zebras, and log movement patterns of the zebras. Research base stations mounted on cars which move around sporadically monitor the data from these movements. When two zebras meet, the corresponding sensors exchange collected data for a potential data delivery back to research base stations.

Brewer et al. [4] proposed DakNet. DakNet is a wireless ad hoc network that has the capacity to provide asynchronous Internet access to remote rural residents using motorcycles and buses to carry users email and web search messages.

Burleigh et al. [5] introduced Inter-planetary network (IPN). IPN is a deep space network of regional Internets. An example of regions includes the terrestrial Internet as a region or a ground-to-orbit region. IPN aims to achieve end-to-end communication through multiple regions in disconnected, variable-delay environments.

2.2 Routing in DTN

Jain et al. [6] introduced and modeled an architecture of a sparse network constituted by fixed sensors and extended by mobile nodes called MULEs (Mobile Ubiquitous LAN Extensions). The MULE architecture involves a very simple and extremely lightweight data routing protocol for the sensors because sensors are the bottleneck of the system. The MULE architecture does not require any synchronization or location information. MULEs move in the network area according to a random mobility model. Their task is to collect data from sensors, buffer them and drop them off later to a set of fixed base stations representing data sinks.

Zhao et al. [7] introduced a controlled-contact routing mechanism that is based on a proactive approach. The approach is termed proactive in the sense that the trajectories of the special mobile nodes, termed as message ferries (MF), are already determined and fixed. Under the assumption of mobility of network nodes,

the authors consider two schemes of messages ferries, depending on whether nodes or ferries initiate the proactive movement. In the Node-Initiated Message Ferrying (NIMF) scheme, ferries move around the area according to known routes, collect messages from the nodes and deliver the messages later to their corresponding destinations. In the Ferry-Initiated Message Ferrying (FIMF), the ferries will move upon service requests to meet the nodes.

Vahdat et al. [8] proposed an epidemic routing protocol which is basically a flooding mechanism accommodated for mobile wireless networks. It relies on pair-wise exchanges of messages between nodes as they get in contact with each other to eventually deliver the messages to their destinations.

Davis et al. [9] considered history-based routing in sparse mobile networks. The objective of their work is to study the impact of different buffer management techniques on an extended variant of the epidemic protocol For the buffer management, they used likelihood meeting values for every other nodes which is based on the history of node contacts.

2.3 Inter-Contact Time between Mobile Nodes

As opposed to extensive research works that have analyzed the properties of mobility models, there are a few works that have addressed the properties of inter-contact times between two mobile nodes or between a mobile and a fixed node.

By using Markov chain to model the data dissemination process between two whales or to model the offloading process between a whale carrying a message and a fixed station, the authors [10] implicitly assumed exponential distributions

for both inter-contact times. They estimated their values using simulations.

Groenevelt et al. [11] showed through extensive simulations that one may accurately model the successive meeting times by Poisson processes when both nodes move according to the same random mobility pattern. They also derived approximation formulas for the intensity of the Poisson processes for both the RWP and the RD mobility models.

Using real traces of six distinct experimental data set, Chaintreau et al. [12] observed that the inter-contact times between two wireless devices carried by humans have a heavy tailed distribution.

Spyropoulos et al.[13] studied the expected meeting times between two mobile nodes, and between a mobile and a static node when mobile nodes are moving according to the RWP and RD models. By considering that the number of travel trips separating two meetings between a pair of nodes is geometrically distributed, the authors provided closed form and approximated expressions for the expected meeting times.

2.4 Power Saving in Wireless Networks

Existing power management protocols for different wireless environments, MANET, Wireless Sensor Networks (WSN), and DTN are presented in this section.

Considering mobility of nodes, the power management mechanisms in MANET are presented in different categories. They are wake-up on-demand based [14] and coordinator based [15].

WSN is a wireless network with distributed autonomous sensors to cooperatively

monitor physical or environmental conditions. Replacing or recharging exhausted batteries is impractical in most WSN scenarios. Some examples of power management mechanisms are presented in [16], [17], and [18] to maximize the network lifetime.

However, existing power saving mechanisms in MANET and WSN assume dense deployment and low mobility of nodes. Therefore, existing power saving mechanisms rely on well connected nodes with few disconnections and disruptions, and cannot be directly applied to DTN.

Several researchers proposed power saving mechanisms in IEEE 802.16e [19] system. For adaptive power saving mechanisms in IEEE 802.16e system, the initial-sleep window and final-sleep window are adjusted according to the average traffic overload or remaining energy state in [20], [21], and [22]. However, it is assumed that communication channel is always available.

A knowledge based framework in sparse connected DTN networks is presented by Jun et al. [23]. In the zero knowledge scenario, assuming a synchronized clock, periodical beacon interval is determined by finding the maximum interval that satisfies the traffic load requirement. In the partial knowledge scenario, searching intervals are estimated using mean and variance values of contact durations and waiting times. However, such statistical information may not be readily available in many real life scenarios.

2.5 Performance of DTN

Guo et al. [24] presented a new kind of delay tolerant network where each node owns a dedicated pigeon/messenger. Specifically, they examined the impact of message batch size on the system performance.

DTN based on the vehicular communications which is referred to as vehicular delay tolerant network (VDTN) was considered by Niyato et al. [25]. The performance of a mobile router in a vehicle was studied by formulating the queueing model. The transmission resources of a mobile router are shared among multiple traffic sources. In this analytical model, the behavior of the traffic source in a competitive environment was also studied.

Wang et al. [26] introduced a generic queuing analytic model for delay/fault-tolerant mobile sensor networks (DFT-MSN) which aims at providing an insight into the queuing characteristics for DFT-MSN with various data delivery schemes and mobility patterns. These authors found that each individual sensor can be approximated as an $M/M/1/K$ queue and the whole network can be treated as a network of queues.

However, the current literature on DTN performance does not consider the buffer management and the power saving together. In addition, the impact of node mobility on the queueing performance and power saving in DTN was not considered.

2.6 Performance of MANET

The performance of multimedia traffic have been tested in various network conditions. Shen et al. [27] proposed an analytical framework for evaluating the quality of service (QoS) of TCP-Friendly Rate Control protocol (TFRC) in hybrid wireless/wired networks. For the wireless network, a link-level truncated Automatic Repeat reQuest (ARQ) scheme is deployed to reduce the packet losses visible to the transport layer protocol. The network performance was analyzed in terms of wireless link utilization, flow throughput, packet loss rate, and probability of end-to-end delay exceeding a prescribed threshold.

Park et al. [28] developed a two-phase loss differentiation algorithm, which captures both collisions and transmission errors for cross-layer optimization to improve the performance of transport layer protocols (e.g., TFRC and TCP) over IEEE 802.11 WLANs.

Eshghi et al. [29] proposed a modified IEEE 802.11 WLAN to support real-time traffic in ad hoc mode by limiting the number of retransmission time fragments. The system performance, such as throughput, delay and probability of fail to deliver were measured. However, this paper as well as the previous two, [27] and [28], focused on MAC layer issues or poor channel conditions, such as fading and shadowing.

The performance of mobile ad hoc networks also has been studied through simulations for the common mobility models in [30], [31], [32], [33], and [34]. In the simulations, node mobility including both node location and moving speed is implemented as pseudo-random events with certain probability distributions. However, the weakness of such simulation based evaluation methodology is the

requirement of huge computing power to achieve the statistics of steady state performance.

Tan et al. [35] presented performance results of differentiated service in MANET through priority buffer management. Based on a similar framework, Dong et al. [36] added the MAC delay and packet collision probability metrics to perform preferential packet dropping/marking schemes to support QoS of real-time traffic. However, the paper assumed a Rayleigh-fading channel as a network parameter.

2.7 Node Mobility

An effort to measure the degree of mobility was made by Kwak et al. in [37]. This measure has a linear relationship with the rate of link change in the network. This makes it useful to measure the performance of various routing protocols under different mobility models. The physical dimensions of the network and the number of nodes were also considered as parameters influencing mobility in addition to the velocity of nodes and transmission range.

The properties of common mobility models were also studied in opportunistic network (ON). The relative velocities for common mobility models are used to analyze inter-contact times of mobile nodes in [38] and [39]. It is shown that the inter-contact times in these mobility models can be closely approximated as exponential distribution under opportunistic network conditions. In opportunistic network, the node behavior in the transmission range is not considered since the transmission area is insignificant compared to the distance of nodes and can be ignored.

The period of time that a route is available between source and destination pair is called route duration or path duration. The first attempt to formulate path duration analytically was made by Sadagopan et al. [40]. By using simple analytical models and with the case study of Dynamic Source Routing (DSR) protocol, the correlation between average path duration and the throughput and reactive routing protocols was established. Han et al. [41] developed a model to explain the exponential distribution for path duration based on hop length.

Chapter 3

Performance Analysis of a Mobile Node

3.1 Introduction

Recently, researchers have considered many power saving mechanisms. However, they mainly have considered how to maximize the throughput performance. Moreover, there have been limited studies for the mechanism of power saving in DTN and the current literature on DTN research does not consider the buffer management and power saving at the same time.

In this thesis, we consider power saving and buffer management together in order to develop an adaptive power management framework that minimizes power consumption and also minimize the performance degradation of buffer management for a mobile node. The adaptive power saving mechanism is based on sleep

scheduling of mobile nodes in MAC layer. In this chapter, we propose a MAC protocol that supports the adaptive sleep scheduling mechanism and we also develop an analytical model to obtain the performance of power saving and queue management.

For the tractable scheduling of the sleep intervals of mobile nodes, a time slot frame based MAC protocol is proposed. A mobile node (MN) decides to sleep or be awake at the beginning of the frame according to the condition of network resources and decides the sleep intervals as multiples of the default beacon interval. According to the different increment method of sleep intervals three different power saving schemes are proposed. The proposed MAC protocol also describes scheduling of the channel access between multiple mobile nodes in the contact range of a source node (SN) or destination node (DN). In the literature of frame based MAC protocols, users contend for every packet transmission. In order to reduce collisions in channel access and to improve the transmission throughput, we consider multiple packets transmission in a frame with one channel access scheduling.

We analyze the proposed sleep interval scheduling schemes to investigate the relation between power saving and queueing performance of a mobile node. Through the model, we first investigate exact amount of power saved by adopting a sleep scheduling mechanism. Then, we also investigate the impact of different sleep intervals on power saving and queueing performance.

The rest of this chapter is organized as follows: In section 2, we describe the proposed MAC algorithm for power saving. In section 3 and section 4, we present an analytical model of three-dimensional Markov chain for a mobile node. In section 5, we present derived performance metrics from the analytical model. The numerical results of analytical models are given in section 6. The results are summarized in section 7.

3.2 Proposed MAC Protocol for Power Saving in DTN

In this section, General traffic delivery between traffic source and destination without power saving mechanism is described. In DTN, the traffic source and destination do not have a direct transmission path among each other. However, a mobile node is used as a carrier to carry the data from traffic source to destination. We assume that the mobile node moves among locations in the network randomly with a random speed. When a mobile node moves into the transmission range of a traffic source, the traffic source transmits data to the mobile node. This mobile node can travel among places and once it moves into the transmission range of the destination, the mobile node transmits data in its buffer to the destination. The details of our frame structured MAC protocol are described in the following section. In power saving scenarios, two operating mode of nodes are considered: a sleep mode and an awake mode. The details of our proposed awake mode operation in the contact area and sleep/awake mechanism for power saving are described.

3.2.1 Frame Structure and Awake Mode Operation

The channel is time-slotted and the time-slot is denoted by a frame. A frame is composed of four or five sub-parts, as depicted in Figure 3.1 and Figure 3.2.Those parts are for beacon broadcasting, advertising, advertising response, and data transmission. The structure of frames is the same in all areas but the operation of the sub-parts is different according to whether the MN is in SN area or in DN area.

The first part is the beacon broadcasting which is used for the MN to listen to the broadcasted beacon signal from other nodes. The second part of a frame is the advertising window consists of a fixed number W of mini-slots. Prior to the advertising window, each MN in the transmission range of an SN selects a random waiting time in the range $[0, W-1]$. To avoid contention, after its own selected random delay, each MN generates a mini-slot length advertising signal.

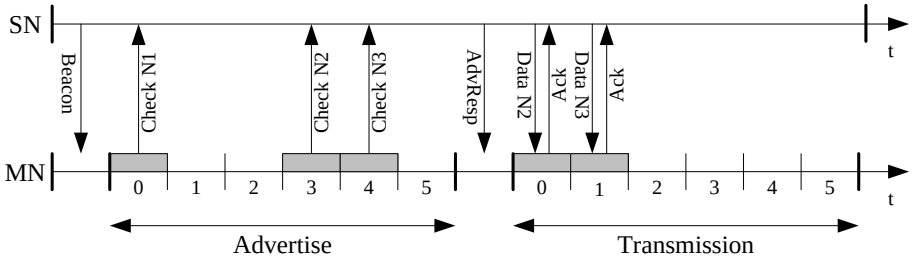

Figure 3.1. Awake mode operation in SN area

In the contact area of SN, through the advertising signal, each MN asks SN if there are packets addressed to the MN in the buffer of the SN. When the advertising of each MN finishes, the SN broadcasts an advertising response message,

which carries a corresponding MN id and slot location for the data that will be transmitted to the MN in the following data transmission window. The SN transmits packets to each MN in sequence at the final part of the frame, the packets transmission window. We assume that all the data packets have a fixed size.

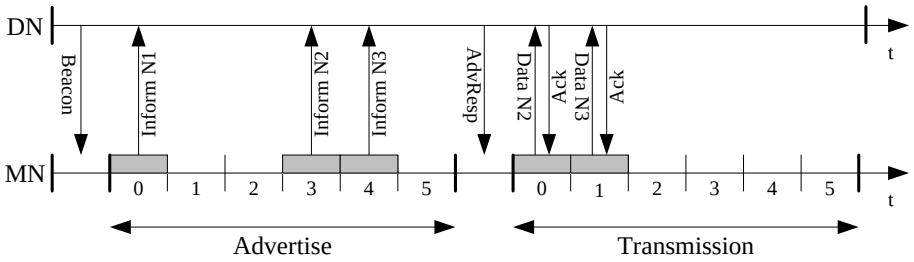

Figure 3.2. Awake mode operation in DN area

In the contact area of DN the random waiting mechanism is the same as in the SN case. In this case, through the advertising signal, if there are packets addressed to the MN in the buffer of the SN, each MN informs DN that there are packets addressed to the DN in the buffer of the MN.

When the advertising of each MN finishes, the DN broadcasts an advertising response message which carries the corresponding MN id and slot location for the data that will be transmitted to the DN in the following data transmission window. Each MN transmits packets to the DN in sequence at the packet transmission window.

In all cases of awake mode, to find out whether a packet has been successfully transmitted or not the receiver sends an acknowledgement (ACK) packet to the sender upon a successful data packet reception at the end of each packet transmis-

sion. If the ACK packet is not received, the packet is regarded as a fail transmission. This ACK mechanism is useful especially when MNs get out of the contact region because the channel can be unavailable during the packet transmissions.

3.2.2 Sleep and Awake Mechanism

In our mechanism, beacon signal is used for an MN to discover the contacts of SN or DN and to synchronize its operation to them. That is, SN and DN periodically broadcast messages called beacons. An MN goes to sleep mode when there is no action required to save energy. If the MN receives a beacon from SN or DN while traveling, it considers that a new contact starts. If it fails to receive the beacons from the corresponding node, the node assumes that the contact is terminated. We assume that nodes have synchronized clocks and can all use a common time period to control when to wake up. Thus MN wakes up during the beacon interval, and continues to check the beacons from SN or DN.

Consider that an MN is out of the contact range of SN or DN, and the MN enters the sleep mode for an interval defined by initial sleep window. When the sleep interval finishes, the MN wakes up and, during the following beacon interval, checks the beacon sinal level again. If the MN is still out of the contact range of SN or DN the MN takes the next sleep interval as defined and returns to the sleep mode.

If the MN receives a beacon from SN or DN, the MN considers that it is in the contact range of corresponding node. In the contact of SN, if there are packets

addressed to the MN in the buffer of the SN, the MN goes to the awake mode and receives the packets from the SN. In the contact of DN, if there are packets addressed to the DN in the buffer of the MN, the MN goes to the awake mode and delivers the packets to the DN. Although the MN is in the contact range of SN or DN, if there is no packets to receive or deliver in the buffer of the MN, the MN returns to the sleep mode. In the following section, we present an analytical model for the proposed power saving mechanism using our MAC protocol and also present the performance analysis results.

3.3 System Description of an MN operation

Figure 3.3 illustrates an MN operation for proposed power saving scheme. The proposed scheme allows local packet arrivals to the MN buffer during sleep periods. In addition, the proposed schemes allow variable length of sleep intervals according to the location and buffer level of the MN.

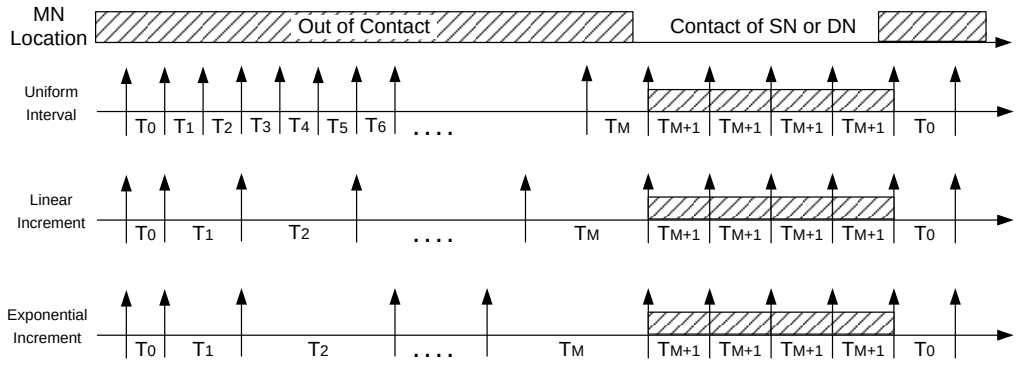

Figure 3.3. Increment Method of Sleep Intervals

The sleep intervals are defined as multiples of the default beacon interval. Accord-

ing to the different increment method of sleep intervals we consider three power saving schemes. T_0 denote the initial sleep interval and the length of the kth sleep interval, T_k, is the kth sleep cycle. The sleep cycle includes a beacon duration but we assume the length of beacon duration is small to be ignored compared to the length of a sleep cycle. The assignment of sleep intervals for each power saving scheme is described as below:

- Uniform Length Scheme: $T_k = T_b$, $0 \leq k \leq M$,
- Linear Increment Scheme: $T_k = (k+1)T_b$, $0 \leq k \leq M$,
- Exponential Increment Scheme: $T_k = 2^k T_b$, $0 \leq k \leq M$,

where, T_b is base interval and M is the final sleep interval index. In addition to the final stage, state (M+1) is a supplementary state named transmission state and is used to describe the packet transmission stage of the SN or MN. Thus, the operation of three schemes is the same in the contact area though each scheme has different sleep interval incrementing method when it is out of the contact area.

3.4 Markov Chain Model

Depending on the location and the buffer state of an MN the MN alters its operating mode. Thus, in order to monitor the state of an MN we analyze the three parameters, the location of MN, the number of packets buffered in the MN, and the sleep/transmission stage of the MN, as a Markov chain model. We assume that the MN residence time in the contact area of SN, DN, and outside of contact

area is exponentially distributed with rate α, β, and γ, respectively. In addition, we assume that the packet arrival process from network to the MN follows a Poisson process with arrival rate λ. The service time of a packet is assumed to be generally distributed. An embedded Markov chain is considered at the following embedded points: immediately before the end of the sleeping period and immediately after the time epoch where an MN packet completes its transmission.

$c(t)$, $b(t)$, and $s(t)$ are set as the stochastic processes representing the location of MN, the number of packets buffered in the MN, and the sleep/transmission stage of the MN at time t. Then, the three-dimensional random process $\{c(t), b(t), s(t)\}$ is an $M/G/1/K$ type discrete-time embedded Markov chain with the state space

$$\Delta = \{(c(t), b(t), s(t)) | c(t) \in \{0, 1, 2\}, 0 \leq b(t) \leq K, 0 \leq s(t) \leq M + 1\}, \quad (3.1)$$

where, K represents the buffer size (in packets) of the MN and the location 0,1,2 corresponds the contact area of SN, contact area of DN area, and out of the contact area, respectively.

To simplify the presentation, the transition probability $P\{c(t+1) = i', b(t+1) = j', s(t+1) = k' | c(t) = i, b(t) = j, s(t) = k\}$ is denoted by $P_{(i,j,k),(i',j',k')}$. Then, the transition probability matrix is given by

$$\mathbf{P} = \begin{bmatrix} \mathbf{P}_{00} & \mathbf{P}_{01} & \mathbf{P}_{02} \\ \mathbf{P}_{10} & \mathbf{P}_{11} & \mathbf{P}_{12} \\ \mathbf{P}_{20} & \mathbf{P}_{21} & \mathbf{P}_{22} \end{bmatrix}$$

where $\mathbf{P}_{i,i'}$ represents the changes of MN location in the network. That is, the MN is in i state in the current time, and the node will be in i' state in the next time. In $\mathbf{P}_{i,i'}$, each element $\mathbf{P}_{(i,j,k),(i',j',k')}$ indicates the transition of the number of

queuing packets from j to j' and the transition of sleep/transmission stage from k to k' when the node location is changed from i to i'.

Due to the Poisson arrival, with mean rate λ, the probability that n packets arrive in time interval T_k is given by

$$P\{N(T_k) = n\} = e^{-\lambda T_k} \frac{(\lambda T_k)^n}{n!}. \tag{3.2}$$

The transition probabilities of sleep/transmission stages are explained in the following. When an MN is in the contact area of SN or DN, if the remaining contact period is greater than current wake-up interval then the node stays in the contact area at the end of wake-up time, otherwise the node moves out of the contact area.

Since the distribution of remaining period is same with the whole distribution of contact period by the memoryless property, the probability of the node stays in the contact area of SN during current wake-up interval T_k is

$$P\{\text{Remaining Contact Period} > T_k\} = e^{-\alpha T_k}. \tag{3.3}$$

Similarly, the probability of the MN moves out of contact area during current wake-up interval T_k is

$$P\{\text{Remaining Contact Period} \leq T_k\} = 1 - e^{-\alpha T_k}. \tag{3.4}$$

The probability for DN is obtained if β is used instead of α.

When an MN is out of the contact area of SN or DN, if the remaining inter-contact period is greater than current sleep interval then the node stays out of the contact area at the end of sleep time, otherwise the node moves into the contact area.

Thus, the probability of the node stays out of the contact area during current sleep interval T_k is

$$P\{\text{Remaining Inter-contact Period} > T_k\} = e^{-\gamma T_k}. \tag{3.5}$$

In addition, the probability of the MN moves into the contact area during current sleep interval T_k is

$$P\{\text{Remaining Inter-contact Period} \leq T_k\} = 1 - e^{-\gamma T_k}. \tag{3.6}$$

Consequently, the transition probability from state (0,n,k) to state (0,n+3,k+1) is the probability that no packets arrive in the kth sleeping state and MN remains SN area until the end of current sleeping period. Then, the transition probability is given by

$$P\{N(T_k) = 3\} \cdot P\{\text{MN remaining in SN area} > T_k\} = e^{-\lambda T_k} \frac{(\lambda T_k)^3}{3!} \cdot e^{-\alpha T_k}$$

Node collision probability can be considered as follows: In awake mode, to avoid contention between nodes in the contact area of an SN or a DN, each MN generates an advertising signal after its own selected random waiting time in the range $[0, W-1]$. A collision occurs when multiple MNs choose the same random waiting number. Thus, the collision probability P_{col} is represented by

$$P_{col} = \sum_{i=2}^{L} \left(\frac{1}{W}\right)^i, L \geq 2, \tag{3.7}$$

where W is the advertising window size in mini-slot and L is the number of MNs in the contact area of an SN, respectively. In this chapter, we assume L is the same with the frame size since the information for the number of MNs in the

contact area of an SN is not given. The collision probability is different according to the number of the MNs as well as the size of frame. The practical collision probability according to the number of MNs will be considered in Chapter 4. If there are collisions between MNs during the advertising time, all the MNs participated in the advertising go to sleep mode during the frame.

We assume SN and DN are located apart far enough so that the contact area of SN and DN is not overlapped each other. Thus, MN does not move directly between SN and DN. The only non-zero one-step transition probabilities for each sub-block are represented as follows:

$\mathbf{P_{00}}$: MN stays in SN

$P_{(0,0,k),(0,0,0)} = P\{N(T_k) = 0\}e^{-\alpha T_k}, \quad k = 0, M+1;$

$P_{(0,0,M+1),(0,0,0)} = P\{N(T_{M+1}) = 0\}e^{-\alpha T_{M+1}};$

$P_{(0,0,k),(0,j',M+1)} = (1 - P_{col})P\{N(T_k) = j'\}e^{-\alpha T_k}, \quad 0 \le j' \le K-1, k = 0, M+1;$

$P_{(0,0,k),(0,j',0)} = P_{col}P\{N(T_k) = j'\}e^{-\alpha T_k}, \quad 0 \le j' \le K-1, k = 0, M+1;$

$P_{(0,0,k),(0,K,M+1)} = (1 - P_{col})\sum_{a=K}^{\infty} P\{N(T_k) = a\}e^{-\alpha T_k}, \quad k = 0, M+1;$

$P_{(0,0,k),(0,K,0)} = P_{col}\sum_{a=K}^{\infty} P\{N(T_k) = a\}e^{-\alpha T_k}, \quad k = 0, M+1;$

$P_{(0,j,k),(0,j-1,M+1)} = (1 - P_{col})P\{N(T_k) = 0\}e^{-\alpha T_k}, \quad k = 0, M+1;$

$P_{(0,j,k),(0,j-1,0)} = P_{col}P\{N(T_k) = 0\}e^{-\alpha T_k}, \quad k = 0, M+1;$

$P_{(0,j,k),(0,j+l,M+1)} = (1 - P_{col})P\{N(T_k) = l+1\}e^{-\alpha T_k}, \quad 0 \le l \le K-j-1, k = 0, M+1;$

$P_{(0,j,k),(0,j+l,0)} = P_{col}P\{N(T_k) = l+1\}e^{-\alpha T_k}, \quad 0 \le l \le K-j-1, k = 0, M+1;$

$P_{(0,j,k),(0,K,M+1)} = (1 - P_{col})\sum_{a=K}^{\infty} P\{N(T_k) = a\}e^{-\alpha T_k}, \quad k = 0, M+1;$

$P_{(0,j,k),(0,K,0)} = P_{col}\sum_{a=K}^{\infty} P\{N(T_k) = a\}e^{-\alpha T_k}, \quad k = 0, M+1.$

P_{02}: MN moves from SN to Outside

$P_{(0,0,k),(2,0,0)} = P\{N(T_k) = 0\} \cdot (1 - e^{-\alpha T_k}), \quad k = 0, M+1;$

$P_{(0,0,k),(2,j',0)} = P\{N(T_k) = j'\} \cdot (1 - e^{-\alpha T_k}), \quad 0 \le j' \le K-1, k = 0, M+1;$

$P_{(0,0,k),(2,K,0)} = \sum_{a=K}^{\infty} P\{N(T_k) = a\} \cdot (1 - e^{-\alpha T_k}), \quad k = 0, M+1;$

$P_{(0,j,k),(2,j-1,0)} = P\{N(T_k) = 0\} \cdot (1 - e^{-\alpha T_k}), \quad k = 0, M+1;$

$P_{(0,j,k),(2,j+l,0)} = P\{N(T_k) = l+1\} \cdot (1 - e^{-\alpha T_k}), \quad 0 \le l \le K-j-1, k = 0, M+1;$

$P_{(0,j,k),(2,K,0)} = \sum_{a=K}^{\infty} P\{N(T_k) = a\} \cdot (1 - e^{-\alpha T_k}), k = 0, M+1;$

P_{11}: MN stays in DN

$P_{(1,0,k),(1,0,0)} = P\{N(T_k) = 0\} e^{-\beta T_k}, \quad k = 0, M+1;$

$P_{(1,0,M+1),(1,0,0)} = P\{N(T_{M+1}) = 0\} e^{-\beta T_{M+1}};$

$P_{(1,0,k),(1,j',M+1)} = (1 - P_{col}) P\{N(T_k) = j'\} e^{-\beta T_k}, \quad 0 \le j' \le K-1, k = 0, M+1;$

$P_{(1,0,k),(1,j',0)} = P_{col} P\{N(T_k) = j'\} e^{-\beta T_k}, \quad 0 \le j' \le K-1, k = 0, M+1;$

$P_{(1,0,k),(1,K,M+1)} = (1 - P_{col}) \sum_{a=K}^{\infty} P\{N(T_k) = a\} e^{-\beta T_k}, \quad k = 0, M+1;$

$P_{(1,0,k),(1,K,0)} = P_{col} \sum_{a=K}^{\infty} P\{N(T_k) = a\} e^{-\beta T_k}, \quad k = 0, M+1;$

$P_{(1,j,k),(1,j-1,M+1)} = (1 - P_{col}) P\{N(T_k) = 0\} e^{-\beta T_k}, \quad k = 0, M+1;$

$P_{(1,j,k),(1,j-1,0)} = P_{col} P\{N(T_k) = 0\} e^{-\beta T_k}, \quad k = 0, M+1;$

$P_{(1,j,k),(1,j+l,M+1)} = (1 - P_{col}) P\{N(T_k) = l+1\} e^{-\beta T_k}, \quad 0 \le l \le K-j-1, k = 0, M+1;$

$P_{(1,j,k),(1,j+l,0)} = P_{col} P\{N(T_k) = l+1\} e^{-\beta T_k}, \quad 0 \le l \le K-j-1, k = 0, M+1;$

$P_{(1,j,k),(1,K,M+1)} = (1 - P_{col}) \sum_{a=K}^{\infty} P\{N(T_k) = a\} e^{-\beta T_k}, \quad k = 0, M+1;$

$P_{(1,j,k),(1,K,0)} = P_{col} \sum_{a=K}^{\infty} P\{N(T_k) = a\} e^{-\beta T_k}, \quad k = 0, M+1.$

$\mathbf{P_{12}}$: MN moves from DN to Outside

$P_{(1,0,k),(2,0,0)} = P\{N(T_k) = 0\}(1 - e^{-\beta T_k}), \quad k = 0, M+1;$

$P_{(1,0,k),(2,j',0)} = P\{N(T_k) = j'\}(1 - e^{-\beta T_k}), \quad 0 \le j' \le K-1, k = 0, M+1;$

$P_{(1,0,k),(2,K,0)} = \sum_{a=K}^{\infty} P\{N(T_k) = a\}(1 - e^{-\beta T_k}), \quad k = 0, M+1;$

$P_{(1,j,k),(2,j-1,0)} = P\{N(T_k) = 0\}(1 - e^{-\beta T_k}), \quad k = 0, M+1;$

$P_{(1,j,k),(2,j+l,0)} = P\{N(T_k) = l+1\}(1 - e^{-\beta T_k}), \quad 0 \le l \le K-j-1, k = 0, M+1;$

$P_{(1,j,k),(2,K,0)} = \sum_{a=K}^{\infty} P\{N(T_k) = a\}(1 - e^{-\beta T_k}), k = 0, M+1;$

$\mathbf{P_{20}}, \mathbf{P_{21}}$: MN moves from Outside to SN or DN

$P_{(2,0,k),(0/1,0,k+1)} = P\{N(T_k) = 0\}(1 - e^{-\gamma T_k})/2, \quad 0 \le k \le M;$

$P_{(2,0,k),(0/1,j',M+1)} = P\{N(T_k) = j'\}(1 - e^{-\gamma T_k})/2, \quad 0 \le j' \le K-1, 0 \le k \le M;$

$P_{(2,0,k),(0/1,K,M+1)} = \sum_{a=K}^{\infty} P\{N(T_k) = a\}(1 - e^{-\gamma T_k})/2, \quad 0 \le k \le M;$

$P_{(2,j,k),(0/1,j,M+1)} = P\{N(T_k) = 0\}(1 - e^{-\gamma T_k})/2, \quad 0 \le k \le M;$

$P_{(2,j,k),(0/1,j+l+1,M+1)} = P\{N(T_k) = l+1\}(1 - e^{-\gamma T_k})/2, 0 \le l \le K-j-2, 0 \le k \le M;$

$P_{(2,j,k),(0/1,K,M+1)} = \sum_{a=K-1}^{\infty} P\{N(T_k) = a\}(1 - e^{-\gamma T_k})/2, \quad 0 \le k \le M.$

$\mathbf{P_{22}}$: MN stays Outside

$P_{(0,0,k),(0,0,k+1)} = P\{N(T_k) = 0\}e^{-\gamma T_k}, \quad 0 \le k \le M-1;$

$P_{(0,0,M),(0,0,M)} = P\{N(T_M) = 0\}e^{-\gamma T_M};$

$P_{(0,0,k),(0,j',k+1)} = P\{N(T_k) = j'\}e^{-\gamma T_k}, \quad 0 \le j' \le K-1, 0 \le k \le M-1;$

$P_{(0,0,M),(0,j',M)} = P\{N(T_M) = j'\}e^{-\gamma T_M}, \quad 0 \le j' \le K-1;$

$P_{(0,0,k),(0,K,k+1)} = \sum_{a=K}^{\infty} P\{N(T_k) = a\}e^{-\gamma T_k}, \quad 0 \le k \le M-1;$

$P_{(0,0,M),(0,K,M)} = \sum_{a=K}^{\infty} P\{N(T_M) = a\}e^{-\gamma T_M};$

$P_{(0,j,k),(0,j,k+1)} = P\{N(T_k) = 0\}e^{-\gamma T_k}, \quad 0 \leq k \leq M-1;$

$P_{(0,j,M),(0,j,M)} = P\{N(T_M) = 0\}e^{-\gamma T_M};$

$P_{(0,j,k),(0,j+l+1,k+1)} = P\{N(T_k) = l+1\}e^{-\gamma T_k}, \quad 0 \leq l \leq K-j-2, 0 \leq k \leq M-1;$

$P_{(0,j,M),(0,j+l+1,M)} = P\{N(T_M) = l+1\}e^{-\gamma T_M}, \quad 0 \leq l \leq K-j-2;$

$P_{(0,j,k),(0,K,k+1)} = \sum_{a=K-1}^{\infty} P\{N(T_k) = a\}e^{-\gamma T_k}, \quad 0 \leq k \leq M-1;$

$P_{(0,j,M),(0,K,M)} = \sum_{a=K-1}^{\infty} P\{N(T_M) = a\}e^{-\gamma T_M}.$

3.5 Performance Analysis

In this section, we describe performance metrics that can be derived from the analytical model. Let $\pi(i,j,k) \equiv \lim_{t\to\infty} P\{((c(t), b(t), s(t))) = (i,j,k)\}$ denote the steady state probability vector for the embedded Markov Chain which satisfies $\pi = \pi P$ and $\pi\mathbf{1} = 1$. The steady state vector for the CTMC of its corresponding embedded DTMC is the proportion of time that the process spends in state (i,j,k) and is given by

$$\pi^*(i,j,k) = \frac{\pi(i,j,k)T_k(i,j,k)}{\sum_{i,j,k} \pi(i,j,k)T_k(i,j,k)}. \tag{3.8}$$

As mentioned in the introduction, the key purpose of employing sleep mode operation in DTN is to conserve the power consumption of MN. To quantify the power saving in the proposed sleep mode operation, two parameters are introduced, contact discovering probability p_{con} and average power consumption P_{avg}. The contact discovering probability p_{con} is defined as the average fraction of the awake time for total operation time and is given by

$$p_{con} = \frac{\sum_{i=0}^{2}\sum_{j=0}^{K} \pi(i,j,M+1)T_k(i,j,M+1)}{\sum_{i=0}^{2}\sum_{j=0}^{K}\sum_{k=0}^{M+1} \pi(i,j,k)T_k(i,j,k)}. \tag{3.9}$$

Energy will be saved at the expense of missed contacts when p_{con} is small, whereas it will be expended when p_{con} is large.

The average power consumption can be computed by the probability sum of the power consumption in each state. Let P_{awake} and P_{sleep} be the average power consumptions in the awake state and the sleep state, respectively. Then, the average power consumption P_{avg} is obtained as following:

$$P_{avg} = \frac{\sum_{i=0}^{2}\sum_{j=0}^{K}\left(\sum_{k=0}^{M}\pi(i,j,k)T_k(i,j,k)P_{sleep} + \pi(i,j,M+1)T_k(i,j,M+1)P_{awake}\right)}{\sum_{i=0}^{2}\sum_{j=0}^{K}\sum_{k=0}^{M+1}\pi(i,j,k)T_k(i,j,k)}. \tag{3.10}$$

Clearly, the smaller the average power consumption, the more efficient the sleep mode operation. For a non-power saving MN, the transceiver is always working and the average power consumption is P_{awake}. Therefore, by comparing P_{avg} and P_{awake} the amount of saved power can be observed by adopting the sleep mode operation.

The rest of metrics are related with the queueing performance of power saving mechanism. Packet loss in the MN buffer occurs if the number of packets reaches the limit of buffer size K. Therefore, the packet loss probability P_{loss} is given by

$$P_{loss} = \sum_{i=0}^{2}\sum_{k=0}^{M+1}\pi^*(i,K,k). \tag{3.11}$$

To obtain the average packet transmission delay mean number of packets in the queue is needed to be calculated. The average queue length for total packets is

given by

$$L = \sum_{j=0}^{K} j \sum_{i=0}^{2} \sum_{k=0}^{M+1} \pi^*(i,j,k). \tag{3.12}$$

The average packet transmission delay is obtained by Little's law as

$$W = \frac{L}{\lambda(1 - P_{loss})}. \tag{3.13}$$

Average Sleep Time is defined as the average time of beacon interval which is in sleep mode and given by

$$S = \sum_{i=0}^{2} \sum_{j=0}^{K} \sum_{k=0}^{M} \pi(i,j,k) T_k(i,j,k). \tag{3.14}$$

The throughput of an MN is defined as the effective packet arrival rate without loss. It is given by

$$T = \lambda(1 - P_{loss}). \tag{3.15}$$

3.6 Numerical Examples

In this section, numerical results are presented to validate and demonstrate the performance of the proposed analytic model. The numerical validation is conducted using MATLAB program. The node contact times and inter-contact time are assumed to have exponentially distributed periods, where the mean periods $\frac{1}{\alpha}$, $\frac{1}{\beta}$ and $\frac{1}{\gamma}$ are set to $10sec$, $10sec$ and $20sec$, respectively. The scenario is considered with the base beacon interval, $T_b = 500msec$, the beacon interval for packet transmission stage, $T_p = 500msec$, and size of MN buffer, $K = 20$. The power consumption values are borrowed from the IEEE IEEE 802.16e because power consumption information of DTN is not given currently. We assume the following power consumption values in each state: $P_{awake} = 750mW$, $P_{sleep} = 50mW$.

Figure 3.4 shows the average power consumption of the exponential increment scheme for different inter-contact times. When the inter-contact time is large the MN stays in the sleep mode long and MN saves more power. If the sleep mode scheme is not adopted then MN is always awake and the average power consumption is $P_{awake} = 750mW$, constant regardless of the packet arrival rate. Thus, the power consumption is significantly reduces when the inter-contact time is large. The average power consumption varies in the range $50mW \sim 250mW$ when the inter-contact time is $20sec$. That is, MN consumes $6.7\% \sim 33\%$ of power compare to that of non-power saving operation. When the inter-contact time is $80sec$, the average power consumption varies in the range $50mW \sim 110mW$ and consumes $6.7\% \sim 15\%$ of non-power saving mode.

Figure 3.5 represents the contact discovering probability of MN for different sleep interval scheduling schemes when the contact time and inter-contact time is fixed for all the schemes. The uniform interval scheme shows higher contact discovering probability than other schemes since this scheme more frequently checks the beacon signal than other schemes.

Figure 3.6 show the average power consumption of MN when the contact time and inter-contact time is fixed for all the schemes. The exponential increment scheme consumes the least power because it has the lowest contact finding probability and has more opportunities to stay in sleep mode. Figure 3.5 and Figure 3.6 shows the tradeoff relation between power consumption and contact discovering probability. Thus, power consumption can be reduced by the choice of longer sleep interval scheme. Figure 3.6 also shows that the power consumption of MN with higher packet arrival rate is more than that of MN with lower packet arrival rate. Higher packet arrival rate makes system utilization larger, so the total awake

time becomes longer.

Figure 3.7 represents throughput for each scheme. The result shows there is only slight throughput performance degradation as the sleep interval increases.

Figure 3.8 show the packet loss probability. Longer sleep interval rate scheme shows slight higher loss probability than others. However, the level is not quite different between the proposed schemes in the effective low range of loss probability.

From Figure 3.7 and Figure 3.8 we can see that with the longer sleep interval scheme lower power consumption can be achieved without packet loss and throughput degradation. The results of throughput and packet loss for different inter-contact times in Figure 3.4 also follow Figure 3.7 and Figure 3.8 because there are no data transmitting actions when MN is out of the contact area.

Figure 3.9 is the mean packet delay in the MN buffer. The exponential increment scheme has the highest packet delay because it has the lowest packet transmission opportunities. Whereas there is not much difference in packet loss between sleep interval schemes, delay performance shows somewhat difference between proposed sleep interval schemes. However, if there is no message loss delay is not a significant problem since this network is for the service that is tolerant for delay.

Figure 3.10 and Figure 3.11 show the performance results for the linear increment scheme, which is tested with three different final sleep interval index, M: 4, 16, and 32. Similarly, Figure 3.12 and Figure 3.13 show the performance results for the exponential increment scheme, which is tested with three different sleep sensing interval index, M: 2, 4, and 6. Both results show the packet loss increase when the final sleep interval index M increases.

3.7 Summary

In this chapter, an adaptive power saving mechanism was designed that minimizes power consumption while maintaining the throughput performance of MN. In addition to the throughput performance, the queueing performance of the MN for the proposed beacon schemes is evaluated and compared. In summary, there is no significant performance difference between beacon schemes, thus it is effective to choose a scheme which has lower beacon rate, but it is not necessary to increase the final sensing interval index to cause packet losses.

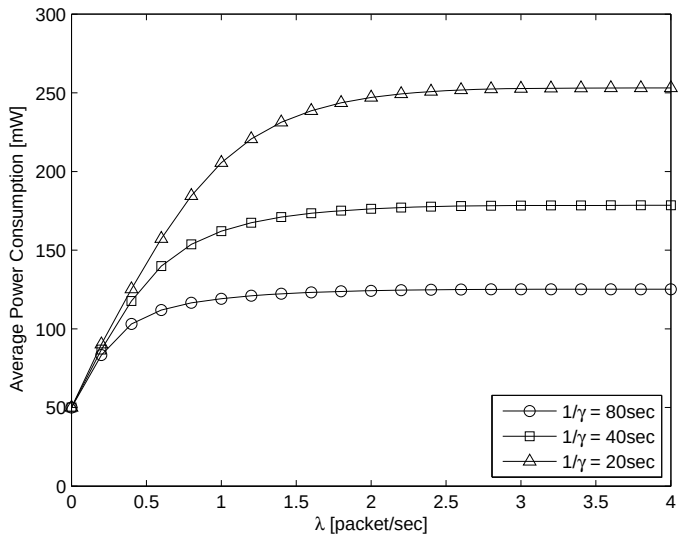

Figure 3.4. Average Power Consumption when $M = 4$.

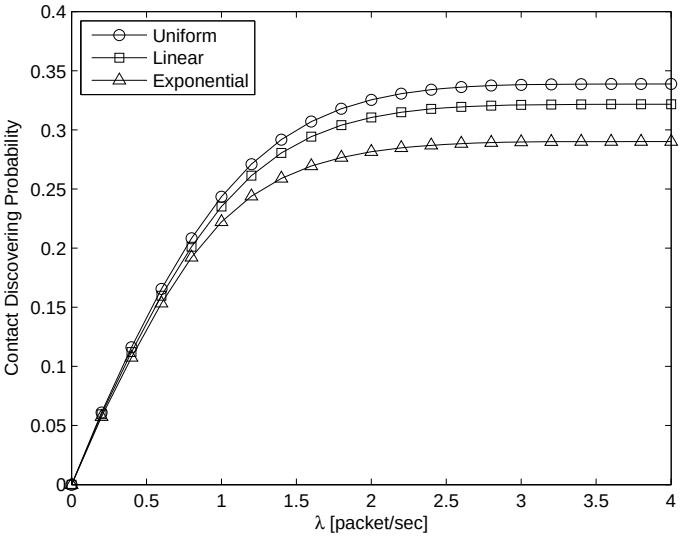

Figure 3.5. Contact Discovering Probability when $M = 4$.

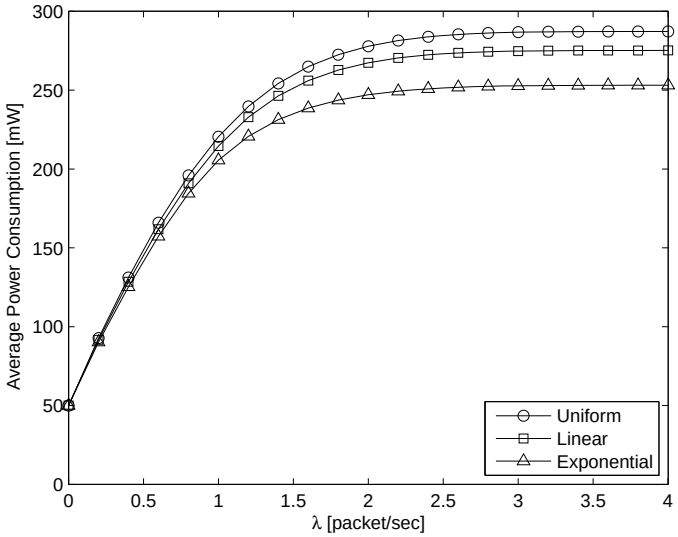

Figure 3.6. Average Power Consumption when $M = 4$.

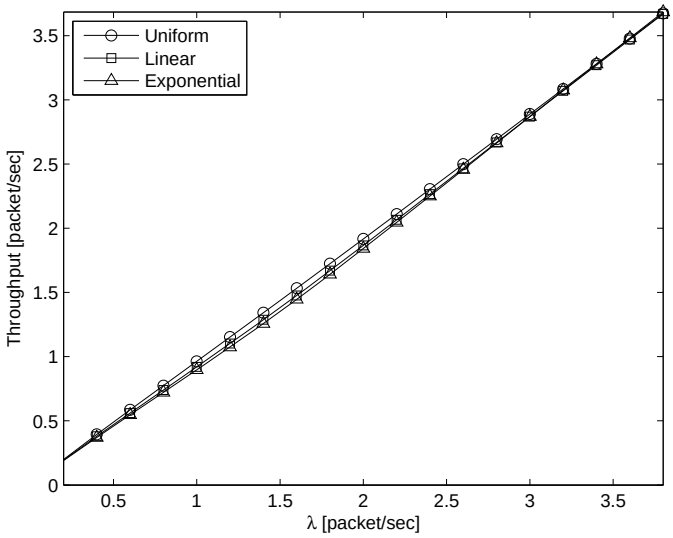

Figure 3.7. Throughput when $M = 4$.

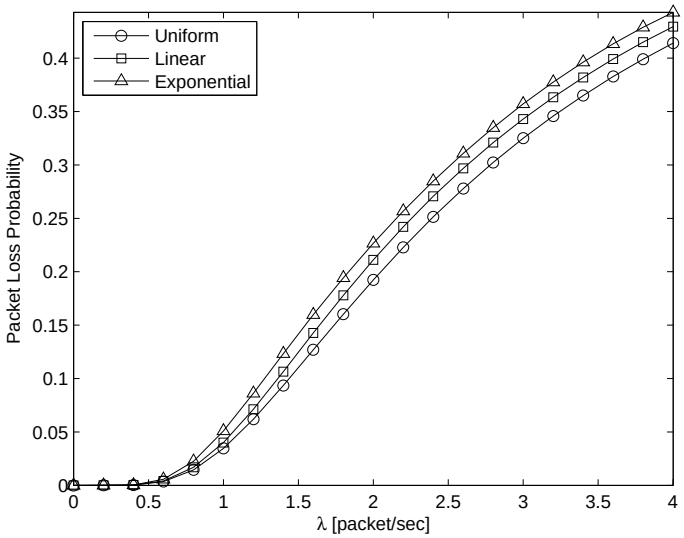

Figure 3.8. Packet Loss Probability when $M = 4$.

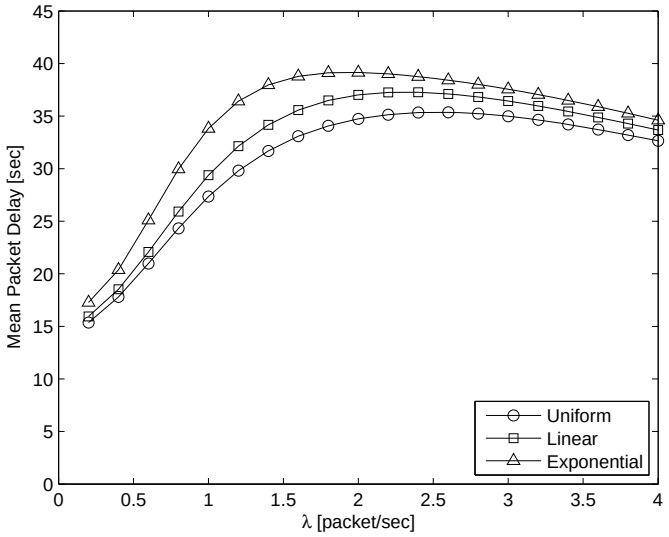

Figure 3.9. Mean Packet Delay when $M = 4$.

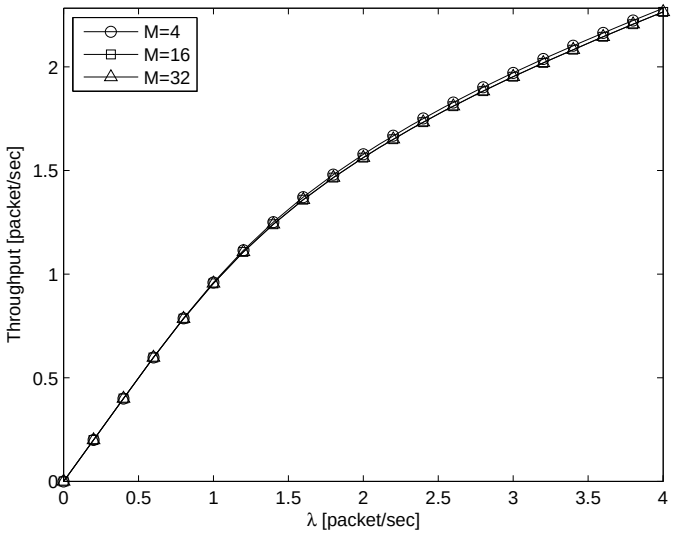

Figure 3.10. Throughput for the linear increment scheme.

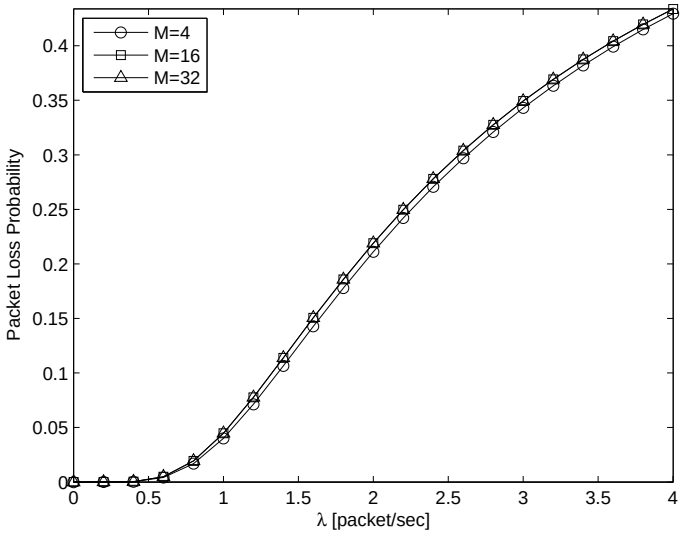

Figure 3.11. Packet Loss Probability for the linear increment scheme.

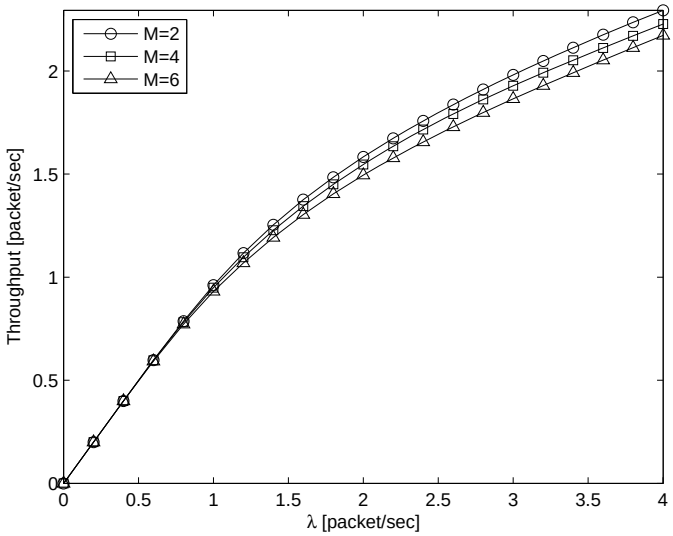

Figure 3.12. Throughput for the exponential increment scheme.

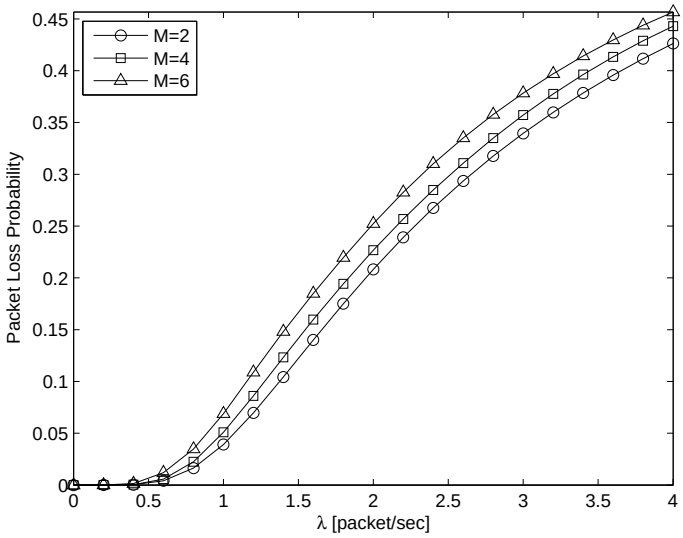

Figure 3.13. Packet Loss Probability for the exponential increment scheme.

Chapter 4

Performance Analysis of a Source Node

4.1 Introduction

In Chapter 3, an adaptive power management framework based on the MAC layer operation is developed. In the framework, power saving and buffer management are considered together to minimize power consumption and performance degradation of buffer management for a mobile node. Through the analytical model, we observed power consumption is significantly reduced by employing a sleep scheduling while maintaining queueing performance of the mobile node. In this chapter, an analytical model for a traffic source node is developed to investigate variations of the performance which are affected by diverse network parameters, such as MAC protocol and node mobility parameters.

As the data delivery mechanism is described in Chapter 3, MNs carry data from traffic sources to destinations since there are no direct transmission paths among the traffic sources and destinations in DTN. In this research, multiple MNs are assumed traveling among locations in the network. It is also assumed SN packets can be delivered to the DN by any MN and SN transmits one packet for each MN in a frame. Therefore, when MNs move into the contact area of an SN, if there are packets addressed to the MNs in the buffer of the SN, corresponding MNs go to the awake mode and the SN transmits data to each MN in sequence.

Unlike MN analysis in Chapter 3, power is not a scarce resource in SNs or DNs because in this research those nodes are assumed to be fixed and the power is supplied from other resources. However, when an SN transmits data to each MN the number of packets that can be transmitted in a frame is limited by the maximum frame size. Therefore, in the performance analysis of an SN we have to consider the number of packets that can be transmitted according to the number of MNs in the contact area of an SN. As in MN analysis, collision between MNs should be also considered in SN analysis because SN does not transmit packets when there is a collision between MNs and the collision is affected by the number of the MNs.

In this chapter, we analyze the queueing performance of an SN for the proposed MAC protocol. Two-dimensional discrete time semi-Markov chain is considered for the number of MNs in the contact area of the SN and the buffer level of the SN. The number of MNs in the SN area is directly associated with MN's arrival rate. With different node's arrival rate, the number of MNs in the steady state

becomes different, which will affect the queueing performance of the SN. Since the MN's arrival rate at the SN is determined by the MN's mobility parameters, we can observe the impact of node mobility on queueing performance of the SN. In Chapter 5, we present how to derive the node arrival rate from node's mobility parameters, such as node velocity, radio transmission range, and node density in the network.

Packet loss, throughput, and average packet delivery delay are considered in the SN as performance measures. Through numerical examples, we examine the impact of MAC parameters, node mobility, and traffic rate on the performance of the SN. Using the analytical results, the system parameters can be optimized while satisfying the QoS constraint. Admissible buffer size of the SN and admissible mobility parameters of the MN that satisfy QoS requirements are determined. From the results of the analysis of MN and SN, the end-to-end performance of DTN is also examined.

The rest of this chapter is organized as follows. In section 2, we present an analytical model of two-dimensional discrete time Markov chain for the number of MNs in the SN area and buffer level of the SN. In section 3, we present performance metrics of the analytical model. The numerical results of analytical models are given in section 4. The results are summarized in section 5.

4.2 Markov Chain Model

Each MN arrival process and the packet arrival process from network to the SN is assumed to follow a Poisson process with arrival rate λ_n and λ_p, respectively. A discrete-time embedded Markov chain is considered at the following embedded points: immediately before the end of the beacon period, immediately after the time epoch where an MN completes its departure from the SN area, and immediately after the time epoch where an SN packet completes its transmission.

$X(t)$ is set to the number of MNs in the contact area of an SN and $J(t)$ is set to the number of packets in the SN buffer at time t. An $M/M/1/K$ type queue is assumed for the SN buffer. Let $X_n = X(t_n+), n = 0, 1, 2, \ldots$ and $J_n = J(t_n+), n = 0, 1, 2, \ldots$. Since t_n is the completion time of the nth departure of an MN, X_n is the number of MNs in the contact area of an SN, immediately after the nth departure completion. J_n represents the number of packets in the buffer immediately after the nth service completion. Also, it is observed that $\{(X_n, J_n) : n = 0, 1, 2, \ldots\}$ is a Markov process with state space $\{0, 1, 2, \ldots, N\} \times \{0, 1, 2, \ldots, K\}$, where N and K represent the limit of the number of MNs and buffer size (in packets) of the SN, respectively.

Now we consider two additional conditions for more realistic analysis. Those are selection probability and collision probability of MNs. Before the collision probability is considered it is needed to limit the number of MNs that can participate in advertising during a frame time of MAC operation. SN packets are assumed to be delivered to the DN by any MN and SN transmits one packet for each MN in

a frame. Thus, if n MNs are in the contact area of SN, SN transmits n packets in sequence in a frame, one for each MN. However, the number of packets that can be transmitted in a frame is limited by the frame size W. That is, if the number of MNs at the current frame is less than or equal to W all the MNs always participates in advertising at the current frame. On the other hand, if n is larger than W at the current frame only W MNs participate in the advertising. An SN is assumed to select the MNs uniformly out of n MNs. Thus, the probability that the selected MNs participate in advertising is

$$P_{sel} = \begin{cases} \frac{W}{n} & \text{if } n > W, \\ 1 & \text{otherwise.} \end{cases} \tag{4.1}$$

Node collision probability was considered when an MN operation is analyzed in Chapter 3. However, in Chapter 3 the number of MNs is assumed to be the same with the frame size since the information for the number of MNs in the contact area of an SN is not given. The collision probability is different according to the number of the MNs as well as the size of frame. In this chapter, practical collision probability is considered according to the number of MNs since the the number of MNs in the contact area of an SN can be traced.

As in Chapter 3, a collision occurs when multiple MNs choose the same random waiting number which is in the range $[0, W-1]$ in awake mode. Thus, when the number of MNs in the contact area, n, is given the collision probability P_{col} is represented by

$$P_{col} = \sum_{i=2}^{L} \left(\frac{1}{W}\right)^i, \quad L \geq 2, \quad L = \begin{cases} n & \text{if } n < W, \\ W & \text{if } n \geq W, \end{cases} \tag{4.2}$$

where, W is the advertising window size in mini-slot. If there are collisions in the advertising part, all the MNs participated in the advertising go to sleep mode during the frame and SN does not transmit data to the MNs. The probability of collision becomes large when n is large and W is set to small.

For the arrival process of MNs and packets, due to the Poisson arrival, with mean rate λ_n, the probability that a_n MNs arrive in time interval T is given by

$$P\{N_a(T) = a_n\} = e^{-\lambda_n T} \frac{(\lambda_n T)^{a_n}}{a_n!} \tag{4.3}$$

and with mean rate λ_p, the probability that a_p packets arrive in time interval T is given by

$$P\{N_a(T) = a_p\} = e^{-\lambda_p T} \frac{(\lambda_p T)^{a_p}}{a_p!}, \tag{4.4}$$

respectively. The departure process in the steady state is also a Poisson process with rate parameter λ_n and λ_p, respectively.

In the two-dimensional transition probability matrix, each element $P_{(i,j),(i',j')}$ indicates the transition probability of number of packets from j to j' when the number of MNs is changed from i to i'. Packet increment and decrement are represented by all possible combinations of packet arrivals and departures. Let a_p, d_p, i_p, and e_p denote the number of packet arrival, departure, increment, and decrement, respectively. The non-zero one-step transition probabilities for the packet increment and decrement are represented in Equation 4.5 and 4.6.

$$\begin{aligned} P_{(n,k),(n,k+i_p)} = P_{sel}(1 - P_{col}) \sum_{a_p=i_p+1}^{K-1-k} P\{N_a(T) = a_p\} P\{N_d(T) = a_p - i_p\} \\ + (1 - P_{sel}(1 - P_{col}))P\{N_a(T) = i_p\}, \quad 0 \le i_p \le K - 1 - k, \end{aligned} \tag{4.5}$$

$$P_{(n,k),(n,k-e_p)} = P_{sel}(1 - P_{col}) \sum_{a_p=0}^{min(n,k)-e_p} P\{N_a(T) = a_p\} P\{N_d(T) = a_p + e_p\},$$

$$1 \leq e_p \leq min(n,k). \quad (4.6)$$

In Equation 4.5, the number of packet increment is $i_p = a_p - d_p$ ($a_p \geq d_p$). Thus, the probabilities of packet increment are represented by the sum of all possible combination of packet arrival and departure probabilities, where n ($0 \leq n \leq N-1$) and k ($0 \leq k \leq K-1$) are current number of MNs in the contact area and current number of packets in the buffer of SN, respectively. In equation, the left term represents packet increment when MNs are selected and there is no collision between them while the right term represents packet increment when MNs are not selected or there is a collision between them. The number of packet arrivals can not exceed the remained buffer capacity and the number of packet departures can not exceed the number of current MNs in the contact area or the frame size W, that is, $(a_p - i_p) \leq L$ ($L = W$ if $n > W$ else $L = n$). If MNs are selected and there is no collision between them packet increment is represented by the differences of packet arrivals and departures. On the other hand, if MNs are not selected or if there is a collision between MNs, packet increment is represented only by the packet arrivals since there is no packet departures.

The number of packet decrement in Equation 4.6 is $e_p = d_p - a_p$ ($d_p > a_p$). The probabilities of packet decrement are also represented by the sum of all possible combinations of packet arrival and departure probabilities. However, packet decrement occurs only when MNs are selected and there is no collision between them. In this case, the number of packet arrivals also can not exceed the remained buffer capacity and the number of packet departures can not exceed the number

of current MNs in the contact area or the frame size W, that is, $(a_p + e_p) \leq L$ ($L = W$ if $n > W$ else $L = n$). If MNs are not selected or if there is a collision between MNs, the number of packets does not decrease since there is no packet departure.

Similarly, the increment and decrement of MNs are also represented by all possible combinations of MN arrivals and departures. Let a_n, d_n, i_n and e_n denote the number of MN arrival, departure, increment, and decrement, respectively. The non-zero one-step transition probabilities for the increment and decrement of MNs are represented in Equations 4.7 and 4.8.

$$P_{(n,k),(n+i_n,k)} = \sum_{a_n=i_n+1}^{N-1-n} P\{N_a(T) = a_n\} P\{N_d(T) = a_n - i_n\},$$

$$0 \leq i_n \leq N - 1 - n, \quad (4.7)$$

$$P_{(n,k),(n-e_n,k)} = \sum_{a_n=0}^{n-e_n} P\{N_a(T) = a_n\} P\{N_d(T) = a_n + e_n\},$$

$$1 \leq e_n \leq n. \quad (4.8)$$

In Equation 4.7, the number of MN increment is $i_n = a_n - d_n$ ($a_n \geq d_n$). However, unlike packet departures, there is no limit to the number of MN departures. All the number of current MNs can depart in a frame duration.

The number of MN decrement in Equation 4.8 is $e_n = d_n - a_n$ ($d_n > a_n$). The probabilities of MN decrement are also represented by the sum of all possible combinations of MN arrival and departure probabilities.

4.3 Performance Analysis

Denote by

$$\pi_{i,j} \equiv \lim_{t\to\infty} P\{(X_n, J_n) = (i, j)\}, \quad i = 0, 1, \ldots N, j = 0, 1, \ldots K$$

the limiting probability of the Markov process $\{(X_n, J_n) : n = 0, 1, 2, \ldots\}$ which satisfies $\pi = \pi P$ and $\pi\mathbf{1} = 1$. Let $\pi_i \equiv (p_{i0}, p_{i1}, \ldots, p_{iK}), i = 1, 2, \ldots, N$, and π_i is the steady state vector for the level of node is i. Thus, the stationary distribution of the Markov process $\{(X_n, J_n) : n = 0, 1, 2, \ldots\}$ is given by

$$\pi = (\pi_0, \pi_1, \pi_2, \ldots, \pi_N).$$

The steady state vector for the CTMC of its corresponding embedded DTMC is the proportion of time that the process spends in state (i, j) and is given by

$$\pi^*(i, j) = \frac{\pi(i, j)T(i, j)}{\sum_{i,j} \pi(i, j)T(i, j)}. \tag{4.9}$$

Packet loss in the buffer of SN occurs if the number of packets reaches the limit of buffer size K. Therefore, the packet loss probability P_{loss} is given by

$$P_{loss} = \sum_{i=0}^{N} \pi^*(i, K). \tag{4.10}$$

To obtain the average packet transmission delay in the SN mean number of packets in the queue is needed to be calculated. The average queue length for total packets is given by

$$L = \sum_{j=0}^{K} j \sum_{i=0}^{N} \pi^*(i, j). \tag{4.11}$$

The throughput and the average packet transmission delay for the SN packets are given by $T = \lambda(1 - P_{loss})$ and $W = \frac{L}{\lambda(1-P_{loss})}$, respectively.

In addition to the packet loss in the SN, we can obtain total packet loss in DTN. Combining the packet loss in MN, total packet loss in DTN is given by

$$P_{loss\_DTN} = P_{loss\_SN} + (1 - P_{loss\_SN})P_{loss\_MN}. \tag{4.12}$$

Total packet delay in DTN is sum of the delay in each MN and SN, and expressed as

$$W_{DTN} = W_{SN} + W_{MN}. \tag{4.13}$$

4.4 Numerical Examples

In this section, numerical examples are given to validate and demonstrate the performance of SN for diverse combination of parameters. We set the base beacon interval, $T_b = 500msec$, the beacon interval for packet transmission stage, $T_p = 500msec$, and size of SN buffer, $K = 20$.

To obtain admissible parameters that satisfy the required QoS constraint, we find parameter pairs that satisfy packet loss probability under a required value ε. That is

$$P\{\text{Packet loss with (parameter1, parameter2) pairs}\} < \varepsilon. \tag{4.14}$$

Figure 4.1, Figure 4.2, and Figure 4.3 represent queueing performance metrics of packet loss probability, packet delay, and throughput for different MN arrival rates. Packet loss and delay are high when MN arrival rate is low because SN packets have less opportunity to be serviced when MN arrival rate is low.

Figure 4.4 and Figure 4.5 show total packet loss and total packet delay in DTN system, respectively. The traffic served in DTN is tolerant for delay. However, delay performance is important to determine the size of data storage which is directly related with the system cost.

It is possible to find minimum buffer size for different packet arrival rates that satisfies a certain QoS requirement. In this thesis, we take the packet loss bound $\varepsilon = 0.05$ in Equation 4.14. Figure 4.6 depicts the admissible region consisting of pairs (K, λ_p) which are the buffer size of SN and the packet arrival rate of SN with required constraint on $P\{\text{Packet loss with } (K, \lambda_p) \text{ pairs}\} < 0.05$. Note that the boundary points of admissible region are the pairs which can be admitted with packet loss bound. In this figure, when λ_p is $1.5 packet/sec$, $K = 3$ is the minimum buffer size that keeps the packet loss probability under 0.05.

In Figure 4.7 the admissible region consisting of pairs (λ_n, λ_p) with required constraint on $P\{\text{Packet loss with } (\lambda_n, \lambda_p) \text{ pairs}\} < 0.05$ is depicted. It shows that in order to keep packet loss rate below 0.05, the packet arrival rate should not be over $1.8 packet/sec$ and $2 packet/sec$ when MN arrival rates are $0.5 node/sec$ and $0.6 node/sec$, respectively. It can also be interpreted in terms of mobility parameters. When the packet arrival rate is $2 packet/sec$, the maximum MN velocity should not be lower than $1.6 m/sec$, which corresponds to an MN arrival rate of $0.6 node/sec$, to keep the packet loss rate below 0.05. The relation of relative velocity, arrival rate, and maximum velocity setting of nodes is depicted in Figure 4.12. Details of the relation is discussed in Chapter 5.

In Figure 4.9, the packet loss probability affected by the frame size W is shown. Packet loss is reduced according to the increment of the frame size because SN has more chances to send packets to MNs when the frame size is large. However, the effect is almost insignificant when the value W is greater than 6.

Figure 4.10 represents collision probability of MNs for different frame window sizes and different number of MNs. The collision probability of MNs is reduced according to the increment of the frame size. Both collision probability and selection probability of MNs are automatically decided in the analytical model according to the number of MNs. Therefore, it is difficult to see the effect on performance by different probability values. In order to see the effect we separately assign those probability values and observe the results in the following. Figure 4.11 and Figure 4.12 show the packet loss probability by MN collision probability and MN selection probability, respectively. However, the actual probability values are too small to change the performance of packet queueing.

4.5 Summary

In this chapter, we evaluated the performance of SN as well as the end-to-end performance of DTN. Based on the analytical results, admissible system parameters, such as buffer size of the SN and arrival rate of the MN, that satisfy given packet loss probability are decided. It means more parameters can be optimized in the same way. For a more exact analysis, selection probability and collision probability of MNs are also considered. However, we observed that the perfor-

mance variation by the collision probability and selection probability of MNs is not significant.

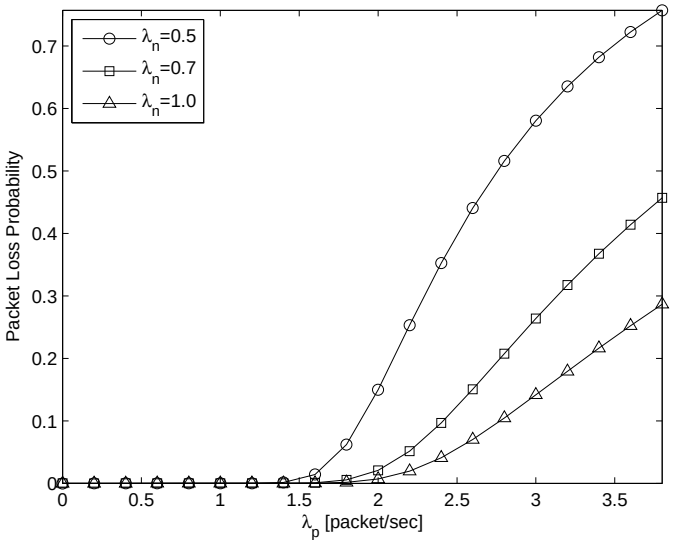

Figure 4.1. Packet Loss Probability ($W = 4$).

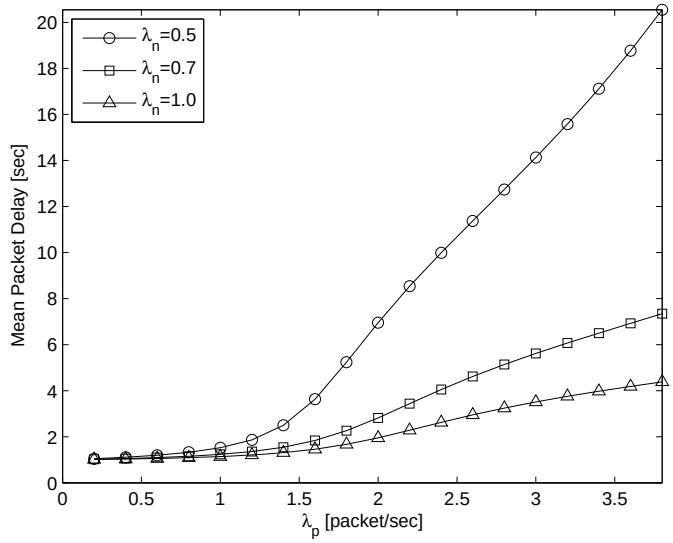

Figure 4.2. Packet Delay ($W = 4$).

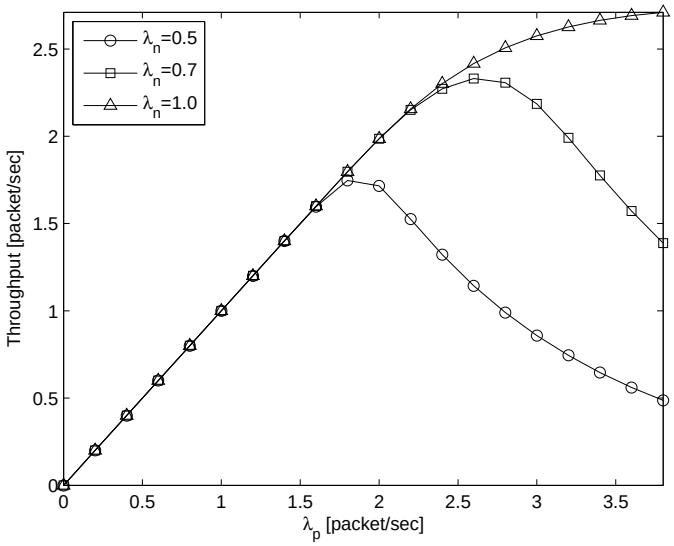

Figure 4.3. Throughput ($W = 4$).

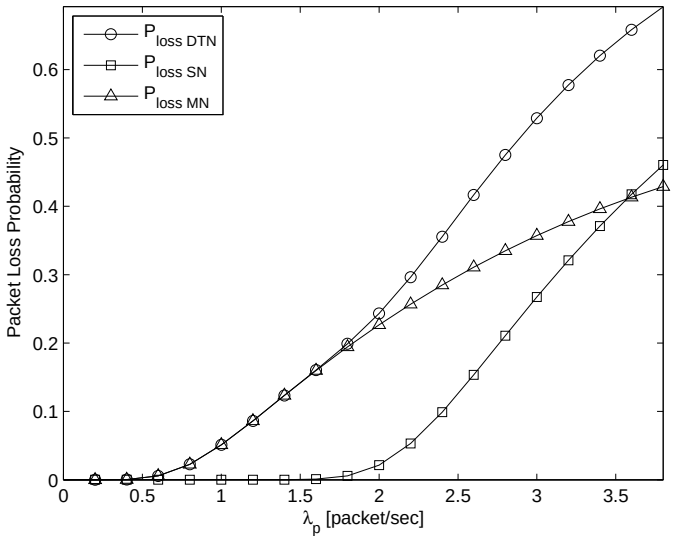

Figure 4.4. Total Packet Loss Probability in DTN ($\lambda_n = 0.8, W = 6$).

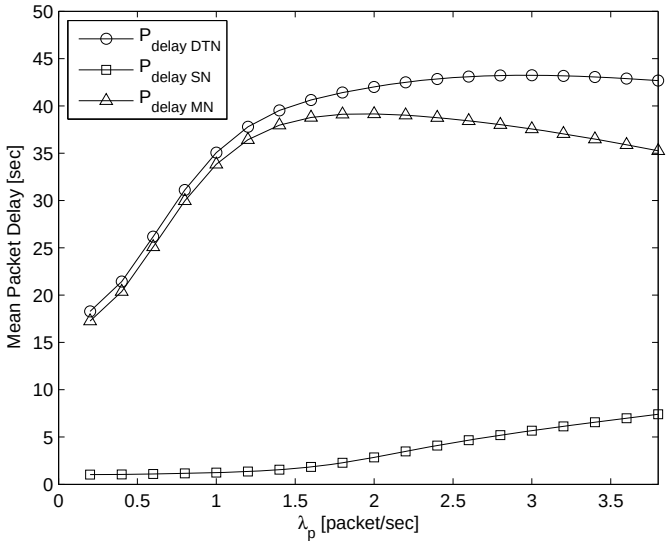

Figure 4.5. Total Packet Delay in DTN ($\lambda_n = 0.8, W = 6$).

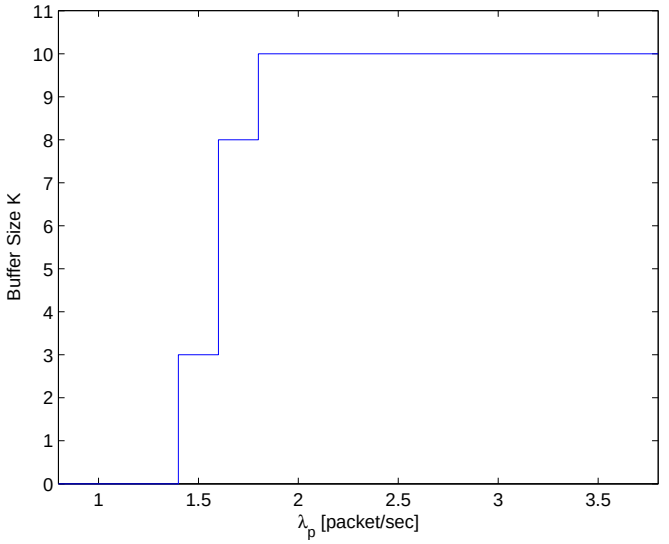

Figure 4.6. Admissible region for $P\{\text{Packet loss with } (K, \lambda_p) \text{ pairs}\} < 0.05$.

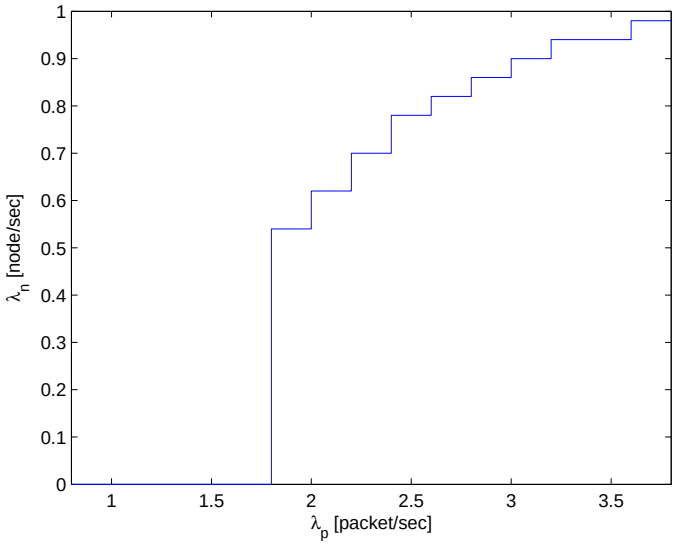

Figure 4.7. Admissible region for $P\{\text{Packet loss with } (\lambda_n, \lambda_p) \text{ pairs}\} < 0.05$.

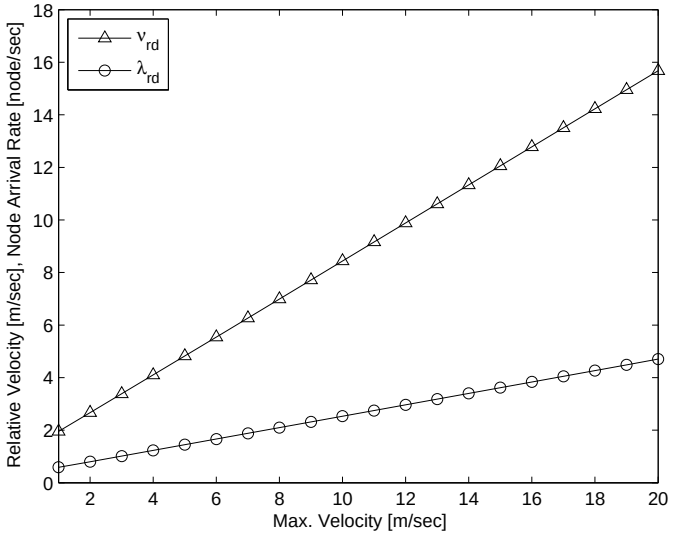

Figure 4.8. MN Arrival Rate and Relative Velocity by v_{max}.

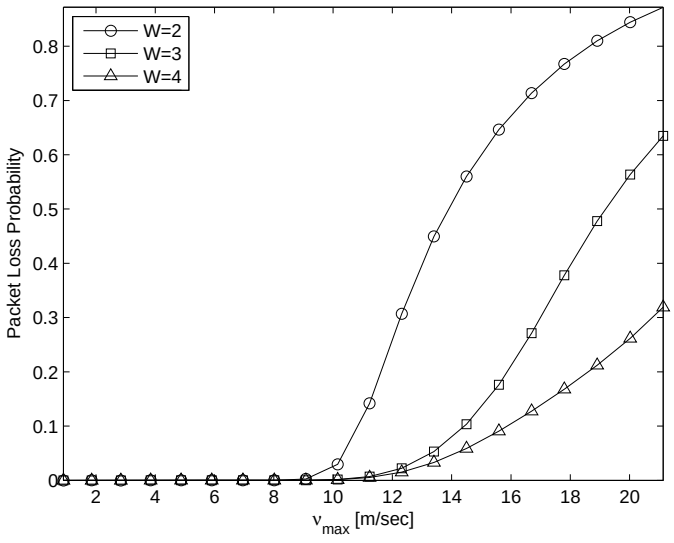

Figure 4.9. Packet Loss Probability by Frame Window Size ($R = 300m$).

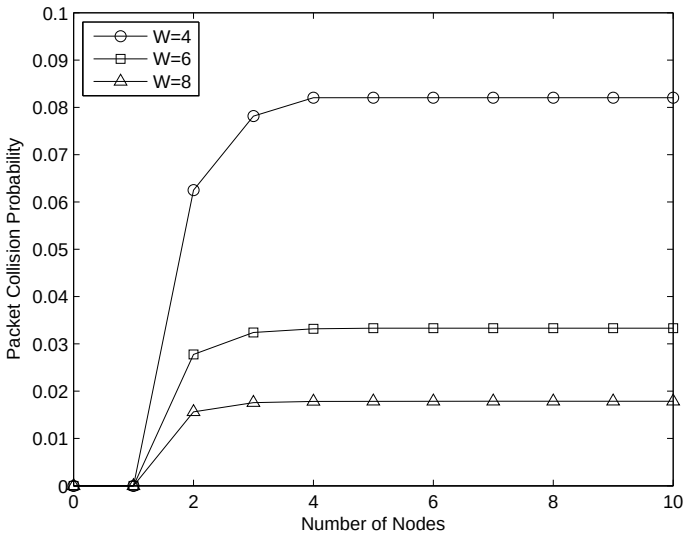

Figure 4.10. Mobile Node Collision Probability.

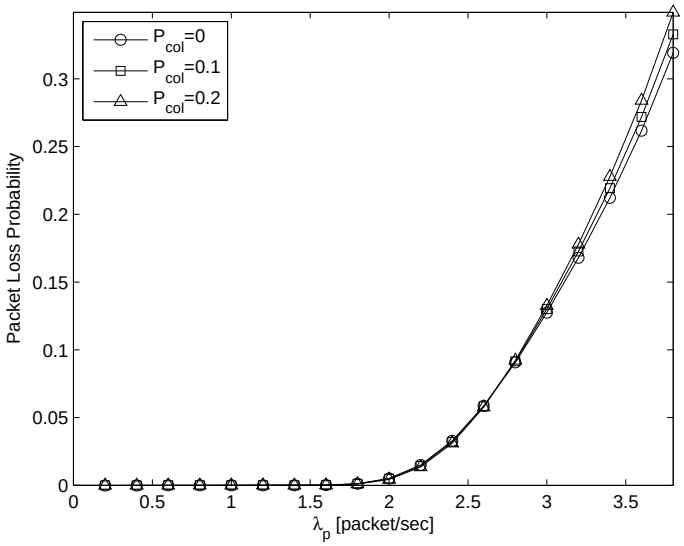

Figure 4.11. Packet Loss Probability by Mobile Node Collision Probability.

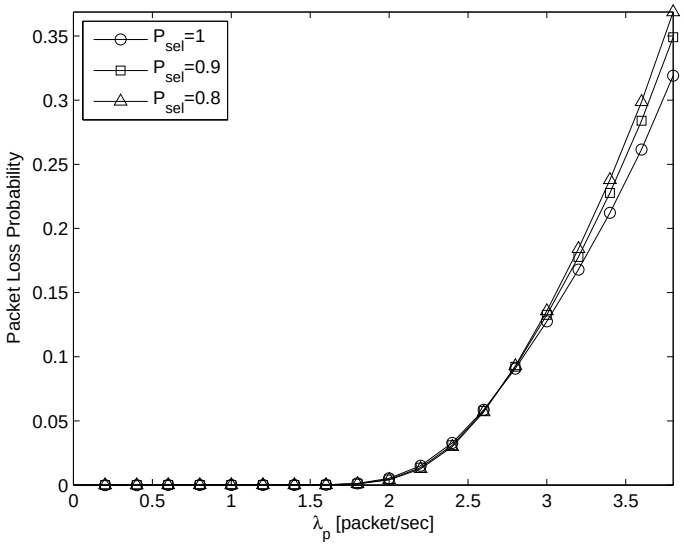

Figure 4.12. Packet Loss Probability by Mobile Node Selection Probability.

Chapter 5

Phase Type Model for Contact Time and Inter-Contact Time

5.1 Introduction

In addition to the important issues in DTN, there are several important parameters, such as contact time and inter-contact time, that greatly affect network performance. In Chapter 3, it was observed that node's contact time and inter-contact time are very important parameters in the performance analysis of power saving mechanism. However, these parameters are assumed to follow exponential distribution and arbitrary numbers are assigned for numerical examples. In Chapter 4, it is also observed that number of nodes in the transmission range of SN affects the performance of data transmission from SN to MN. The number of nodes in the transmission range is directly associated with node arrival rate in the node's transmission range.

In order to reflect more realistic situations, the details of the node arrival rate, contact time, and inter-contact time are investigated in this chapter. These parameters mainly depend on the mobility of the nodes. The mobility can be characterized by network parameters, such as radio transmission distance of a node, node speed, and node density in the network.

First, the node arrival rate, contact time, and inter-contact time are derived from node's mobility parameters rather than assigning arbitrary numbers. Derived parameters allow us to observe the variations of DTN performance by the mobility parameters. For the distribution of node contact time and inter-contact time, there are different arguments as described in the literature review for the inter-contact time in Chapter 2. In the literature, it has shown that the parameters follow exponential distribution, heavy tailed distribution, or other distributions. Thus, we need to investigate the performance of DTN when the contact time and inter-contact time have general distributions. In this research, we express the parameters as PH model. The PH model is flexible, so that most distributions can be represented or approximated by a PH distribution [42]. In addition, the PH model is also tractable to be used in the performance analysis. Finally, using this general model the performance of DTN is analyzed, which has performed using exponential expression of contact time and inter-contact time in Chapter 3. The results is also compared with those of Chapter 3.

The rest of this chapter is organized as follows: In section 2, we describe the derivation of node arrival rate and inter-contact time. We derive node contact

time in section 3. In section 4, we present PH Model for node contact time and node inter-contact time. The numerical results of analytical models are given in section 5. The results are summarized in section 6.

5.2 Node Arrival Rate and Inter-Contact Time

In this section, node arrival rate and inter-contact time are derived from the mobility parameters. To compute the node arrival rate λ for a reference node, the concept of link generation rate and link breakage rate are adopted as in [43], [44]. Consider a network with multiple mobile nodes N_i and a reference node N_0 as shown in Figure 5.1, where all nodes have the same transmission distance of R and move with their own velocity v_i.

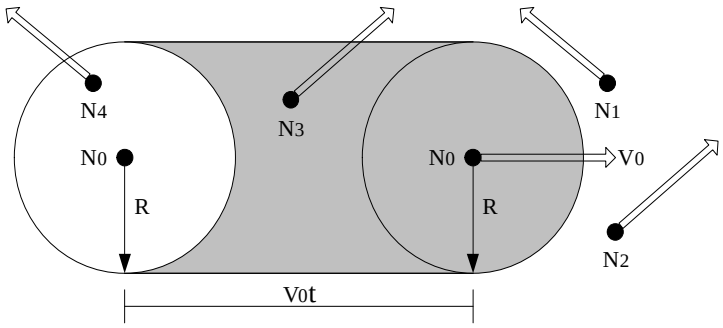

Figure 5.1. Concept of node arrival rate.

As a reference mobile node N_0 is moving on the network plane, its circular communication region sweeps the network plane. If the node moves with a velocity v_0 for time t the swept area is $A_{sweep} = 2Rv_0t$. Therefore, the expected number of nodes entering the area A_{sweep} with velocity v_0 within the next t seconds is $2Rv_0t\sigma$, where σ denotes node density in the network. The rate of total node

arrivals to the reference node is the expected number of nodes entering the transmission area per second. Thus, the average rate of the total node arrival can be expressed by integrating $2R\sigma v_r$ over all possible value of θ.

$$\lambda = \frac{1}{\pi} \int_0^{\pi} 2R\sigma v_r(\theta) d\theta \tag{5.1}$$

where, v_r is the relative velocity between nodes.

The relative velocity v_r is defined by Equation (5.2), considering two nodes N_i and N_j with velocity vectors $\vec{v_i}$ and $\vec{v_j}$, respectively. The relative velocity vector of N_j with respect toN_i is defined as $\vec{v_r} = \vec{v_j} - \vec{v_i}$ with a magnitude of [43]

$$v_r = |\vec{v_r}| \triangleq \sqrt{v_i^2 + v_j^2 - 2v_i v_j cos\theta}, \tag{5.2}$$

where, θ is the relative angle between $\vec{v_i}$ and $\vec{v_j}$, measured counter-clockwise from the direction of $\vec{v_i}$.

The relative velocity can be adapted from the Random Direction (RD) [45] mobility model in order to reflect general and realistic mobility parameters in node arrival rate. The stationary distributions of nodes have been shown to be uniform in the RD model irrespective of the boundaries being reflecting or wrap around [33] whereas nodes are more likely to be concentrated near the center of the area in the RWP mobility model [46].

In the RD model, the destination is chosen uniformly in the finite moving area, and the movement speed v is uniformly chosen from $[v_{min}, v_{max}]$, where $0 < v_{min} < v_{max} < \infty$. The direction θ is uniformly chosen from $[0, 2\pi]$, and the time duration of the travel is chosen from an exponential distribution with average epoch

duration [38]. The velocity and direction are assumed to be independent of each other. Both the velocity and direction change in each epoch but are constant for the duration of an epoch. Therefore, the expected value of relative velocity is given by

$$\bar{v_r} = \int_{v_{min}}^{v_{max}} \int_{v_{min}}^{v_{max}} \int_{0}^{2\pi} v_r f_{V_i V_j \Theta}(v_i, v_j, \theta)\, d\theta\, dv_i\, dv_j. \tag{5.3}$$

where $f_{V_i V_j \Theta}(v_i, v_j, \theta)$ is the joint probability density function (pdf) of v_i, v_j and θ. Let $f_{V_i}(v_i)$, $f_{V_j}(v_j)$ and $f_\Theta(\theta)$ denote the pdf of v_i, v_j and θ, respectively. Since v_i, v_j and θ are independent variables, the joint pdf can be obtained as

$$f_{V_i V_j \Theta}(v_i, v_j, \theta) = f_{V_i}(v_i) f_{V_j}(v_j) f_\Theta(\theta). \tag{5.4}$$

The distribution of relative movement direction is given as $f_\Theta(\theta) = 1/2\pi$ for both mobility models.

In addition, the average velocity of a single node is given in [47] as

$$\bar{v} = \frac{v_{max} + v_{min}}{2}. \tag{5.5}$$

The pdf $f_V(v)$ under RD mobility model is also given in [47] as

$$f_V(v) = \frac{1}{v_{max} - v_{min}}, \quad v_{min} \le v \le v_{max}. \tag{5.6}$$

Thus, the average relative velocity of two nodes is given as follows [38]:

$$\bar{v_r} = \frac{1}{2\pi (v_{max} - v_{min})^2} \int_{v_{min}}^{v_{max}} \int_{v_{min}}^{v_{max}} \int_{0}^{2\pi} \sqrt{v_i^2 + v_j^2 - 2 v_i v_j cos\theta}\, d\theta\, dv_i\, dv_j, \tag{5.7}$$

where θ is the angle between two movement directions.

After arranging the Equations (5.1) $\sim$ (5.7) we have the expected node arrival rate under RD mobility model as

$$\bar{\lambda} = \frac{R\sigma}{\pi (v_{max} - v_{min})^2} \int_{v_{min}}^{v_{max}} \int_{v_{min}}^{v_{max}} \int_{0}^{2\pi} \sqrt{v_i^2 + v_j^2 - 2 v_i v_j cos\theta}\, d\theta\, dv_i\, dv_j. \tag{5.8}$$

The inter-contact time also derived from the node arrival rate since inter-contact time is defined as the time duration between consecutive contacts of node pairs. Therefore, the expected inter-contact time between mobile nodes under the RD model is approximated as

$$\bar{t}_{intc} \approx \frac{1}{\bar{\lambda}} = \frac{\pi(v_{max} - v_{min})^2}{R\sigma \int_{v_{min}}^{v_{max}} \int_{v_{min}}^{v_{max}} \int_0^{2\pi} \sqrt{v_i^2 + v_j^2 - 2v_i v_j cos\theta}\, d\theta\, dv_i\, dv_j}. \tag{5.9}$$

5.3 Node Contact Time

Next, the contact time among mobile nodes is considered. The contact time is derived from the inter-contact time. Let $f(x, y)$ denote the node spatial probability density function for the given node and A_{net} denote the size of the whole network area. The node is assumed to move randomly inside the area A_{net} following uniform distribution. Then, the density function of the random variable that a node i is at an arbitrary location in A_{net} is

$$f(x, y) = \frac{1}{A_{net}}. \tag{5.10}$$

Thus, the probability that a given node will be within a certain area A_{in} in the network is given by

$$P_{in} = \int\int_{A_{in}} f(x, y)\, dx\, dy = \frac{A_{in}}{A_{net}}. \tag{5.11}$$

In a similar manner, the probability that a given node will be outside of the area A_{in} in the network is given by $\frac{A_{out}}{A_{net}}$, where $A_{out} = A_{net} - A_{in}$.

When considering a long enough time interval T, the time spent in area A_{in} for a given node can be obtained as $\bar{t}_{in} = P_{in}T$. In addition, if the time spent out of

the area A_{in} for a given node is considered as $\bar{t}_{out} = P_{out}T$, the $\bar{t}_{in}$ is arranged as

$$\bar{t}_{in} = \frac{P_{in}}{P_{out}}\bar{t}_{out} = \frac{A_{in}}{A_{net} - A_{in}}\bar{t}_{out}. \tag{5.12}$$

Therefore, if a source node which has transmission area A_{in} is considered the contact time of a mobile node for this source node can be obtained as

$$\bar{t}_{cont} = \frac{A_{in}}{A_{out}}\bar{t}_{intc}, \tag{5.13}$$

where $\bar{t}_{intc}$ is the outside area of A_{in} and inter-contact time of nodes, respectively. Consequently, the contact time is expressed as the ratio of network size from inter-contact time.

5.4 Phase Type Model for Contact Time and Inter-Contact Time

In order to capture a general stochastic behavior, we assume that the contact time and inter-contact time of node follow continuous PH distributions. A continuous PH distribution is the distribution of the time to absorption in a finite continuous time Markov chain. The transition probability matrix P of dimension $m + 1$ is given by

$$\mathbf{P} = \begin{bmatrix} \mathbf{T} & \mathbf{t} \\ \mathbf{0} & 0 \end{bmatrix} \tag{5.14}$$

where $\mathbf{T}$ is the $(m \times m)$ matrix grouping the transition probabilities among the transient states, $\mathbf{t}$ is the l-dimensional column vector grouping the probabilities from any transient state to the absorbing one, and $\mathbf{0}$ is a zero row vector.

The contact time of node for SN is assumed to have the PH($\boldsymbol{\alpha}, \mathbf{T}$) distribution of order m, where $\boldsymbol{\alpha}$ is an initial probability vector such that $\boldsymbol{\alpha}\mathbf{1} = \mathbf{1}$. Every

element of $\mathbf{T}$ has the following property; $0 \leq T_{ij} \leq 1$ and $\mathbf{T1} \leq \mathbf{1}$ with at least one of the rows strictly less than 1, where $\mathbf{1}$ is a column vector of ones. In a similar manner, the contact time of node for DN and the inter-contact time of node has the assumed to have the PH$(\boldsymbol{\beta}, \mathbf{S})$ distribution of order m and PH$(\boldsymbol{\gamma}, \mathbf{R})$ distribution of order n, respectively.

The transition probabilities of sleep/transmission stages using PH distribution is described below. In Chapter 3, the probabilities using exponential distribution was obtained. The condition of node movement between contact and inter-contact area is same as in Chapter 3. That is, when an MN is in the contact area of SN or DN, if the remaining contact period is greater than current beacon interval it means the node stays in the contact area at the end of beacon time, otherwise it means the node moves out of the contact area.

In the PH model, the remaining contact period can be expressed using complement of cumulative distribution [48] and the probability of the MN stays in the contact area of SN during current wake-up interval T_k is

$$P\{\text{Remaining Contact Period} > T_k\} = 1 - \boldsymbol{\alpha} e^{\mathbf{T}T_k}\mathbf{1}. \tag{5.15}$$

Similarly, the probability of the MN moves out of contact area during current wake-up interval T_k is

$$P\{\text{Remaining Contact Period} \leq T_k\} = \boldsymbol{\alpha} e^{\mathbf{T}T_k}\mathbf{1}. \tag{5.16}$$

The probability for DN is obtained if PH$(\boldsymbol{\beta}, \mathbf{S})$ is used instead of PH$(\boldsymbol{\alpha}, \mathbf{T})$.

When an MN is out of the contact area of SN or DN, if the remaining inter-contact period is greater than current sleep interval it means the node stays out of the

contact area at the end of sleep time. So, the probability of the node stays out of the contact area during current sleep interval T_k is

$$P\{\text{Remaining Inter-contact Period} > T_k\} = 1 - \boldsymbol{\gamma} e^{\mathbf{R}T_k}\mathbf{1}. \tag{5.17}$$

In addition, the probability of the MN moves into the contact area during current sleep interval T_k is

$$P\{\text{Remaining Inter-contact Period} \leq T_k\} = \boldsymbol{\gamma} e^{\mathbf{R}T_k}\mathbf{1}. \tag{5.18}$$

The only non-zero one-step transition probabilities for PH distribution are represented in the Appendix. Next, the performance of Chapter 3 for PH model is examined.

5.5 Numerical Examples

The node arrival rate λ for different mobility parameters is observed first. In Chapter 4, the node arrival rate λ for different v_{max} settings was shown in Figure 4.8 when $R = 300m$ and $\sigma = 1/2000m^2$. In addition to that, the node arrival rate for different radio transmission range and node density is depicted in Figure 5.2 and Figure 5.3, respectively. The node arrival rate is also proportional to the radio transmission range and node density.

Once the PH model for contact time and inter-contact time is established, it is needed to fit model parameters to the actual distributions. The density functions of contact time and inter-contact time are approximated with PH distributions. First, the density function of node arrival rate is obtained using the closed form

expression of density function for relative velocity given in [49]. Then, through the numerical calculation, the density functions of node contact time and inter-contact time are obtained from the density function of node arrival rate. Figure 5.4 shows the density function of node arrival rate. The obtained density function and distribution function of node inter-contact time are compared with exponential distribution and fitted PH distribution in Figure 5.5 and Figure 5.6, respectively. In the figures, the PH model is more closer to the actual distribution than exponential model.

For fitting PH distributions, existing EMpht program [50] is used. The program is an implementation of the EM (expectation-maximization) algorithm which is an iterative method for maximum likelihood estimation. The order of PH distribution is given by the user and that is selected as 3.

The fitted continuous time PH distribution of node contact time for SN that corresponds to the actual distribution with mean periods $10sec$ is given by PH(α, T), where

$$\alpha = \begin{bmatrix} 0 & 1 & 0 \end{bmatrix}, \quad T = \begin{bmatrix} -0.6612 & 0.0044 & 0.3955 \\ 0.6163 & -0.6298 & 0.0135 \\ 0.0051 & 0.6490 & -0.6655 \end{bmatrix}.$$

The phase type parameter for DN, PH(β, S), is assumed to be the same as that of SN.

The fitted continuous time PH distribution of node inter-contact time is given by

$$\gamma = \begin{bmatrix} 0 & 1 & 0 \end{bmatrix}, \quad R = \begin{bmatrix} -0.3306 & 0.0022 & 0.1977 \\ 0.3082 & -0.3149 & 0.0067 \\ 0.0025 & 0.3245 & -0.3328 \end{bmatrix}.$$

It corresponds to the actual distribution with mean periods $20sec$.

Figure 5.7 and Figure 5.8 compare packet loss and packet delay in MN with respect to different contact time and inter-contact time models. From these figures, it can be observed that the performance by PH distribution is better than that of exponential model.

5.6 Summary

In this chapter, the relation of node arrival rate, contact time, and inter-contact time was examined with node mobility parameters, such as node velocity, radio transmission range, and node density in the network. Then, the node contact time and inter-contact time are also expressed as PH model. Using this general model the performance of mobile node was analyzed, and then the results were compared with those of Chapter 3. It is examined that the PH model is more closer to the actual distribution than exponential model and the performance by PH model is better than that of exponential model.

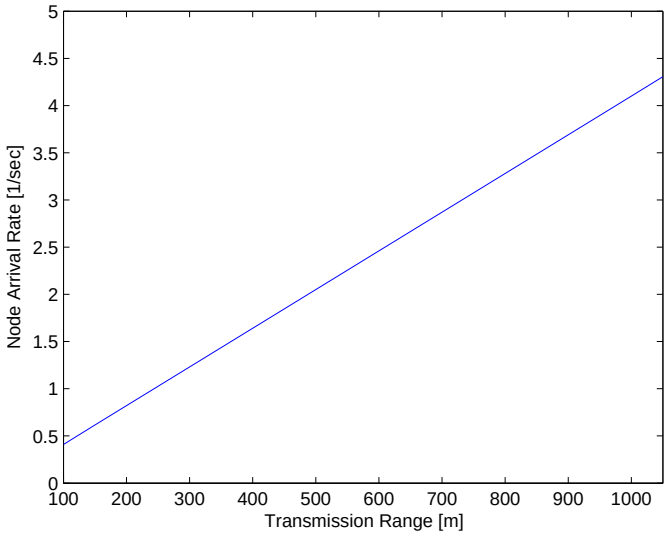

Figure 5.2. Node Arrival Rate ($v_{max} = 5m/sec, \sigma = 1/2000m^2$).

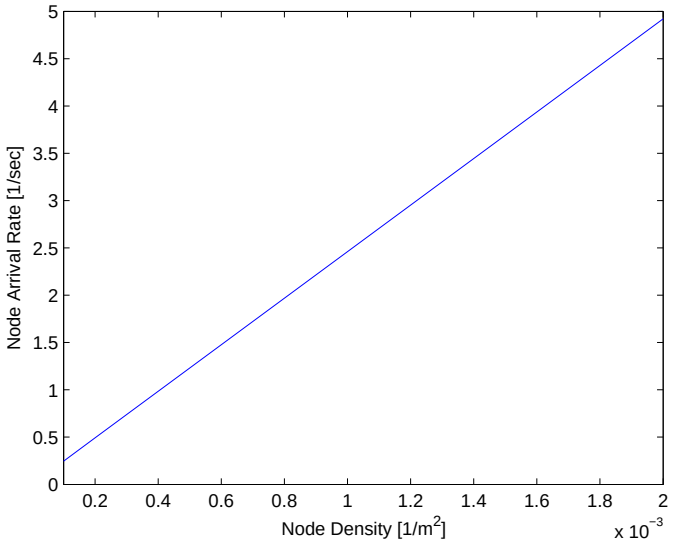

Figure 5.3. Node Arrival Rate ($v_{max} = 5m/sec, R = 300m$).

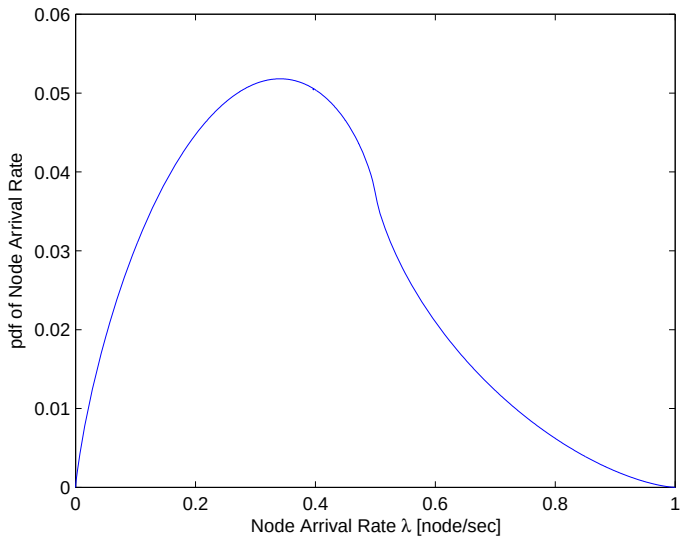

Figure 5.4. pdf of Node Arrival Rate.

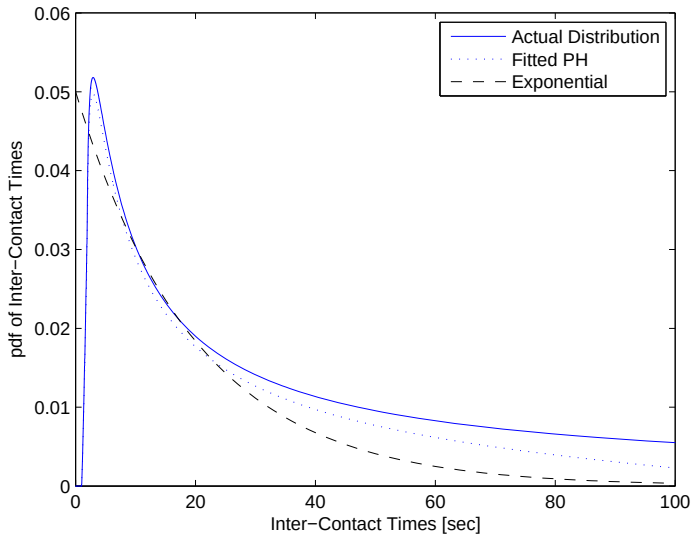

Figure 5.5. pdf of node inter-contact time.

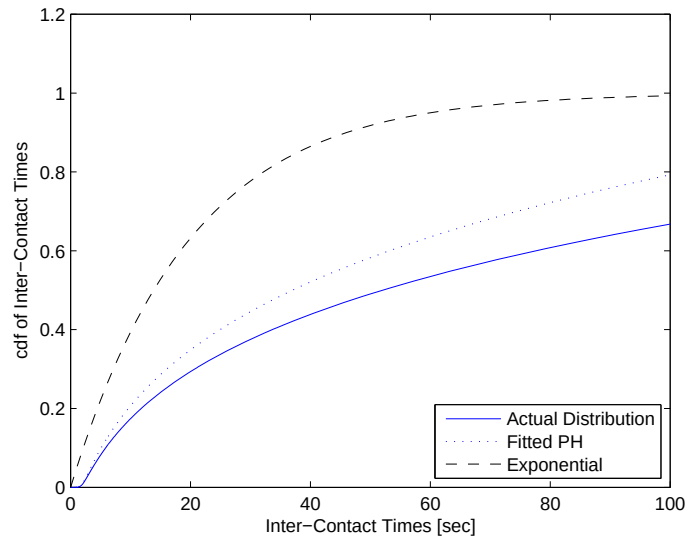

Figure 5.6. cdf of node inter-contact time.

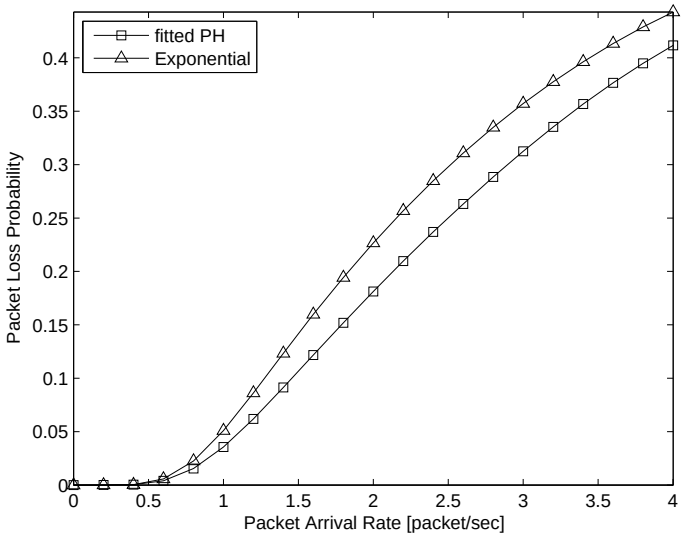

Figure 5.7. Packet Loss Probability when $M = 4$.

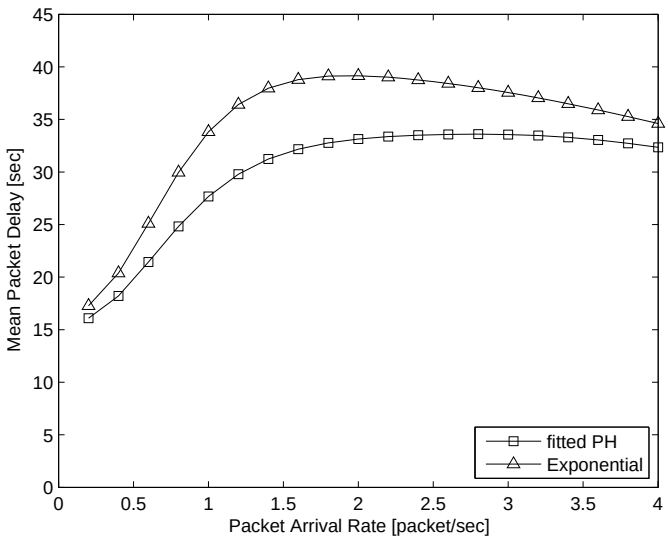

Figure 5.8. Mean Packet Delay when $M = 4$.

Chapter 6

Conclusions and Future Works

In this chapter, the results obtained in this thesis are summarized and some possible directions for future research are presented. In this thesis, a MAC protocol that supports adaptive sleep scheduling of a mobile node is proposed. Based on the MAC layer operation, an adaptive power management framework is developed. The framework considers power saving and buffer management together in order to minimize power consumption while minimizing the performance degradation of buffer management for the mobile node. Through the analytical model, it is examined that power consumption is significantly reduced by employing sleep scheduling while maintaining queueing performance of the mobile node. In addition to the throughput performance, the queueing performance of the MN for the proposed beacon schemes is evaluated and compared. There is no significant performance difference between beacon schemes, thus it is effective to choose a scheme which has lower beacon rate, but it is not necessary to increase the final sensing interval index to cause packet losses.

The performance of SN as well as the end-to-end performance of DTN are also

evaluated. Variations of the performance of an SN are affected by diverse network parameters. Through the numerical example the impact of MAC parameters, node mobility, and traffic rate on packet loss, delay, and throughput is examined. Admissible system parameters, such as buffer size of the SN and arrival rate of the MN, that satisfy given packet loss probability are also decided. For a more exact analysis, selection probability and collision probability of MNs are also considered. However, the performance variation by the collision probability and selection probability of MNs was not significant. The performance of proposed MAC scheme is analyzed by modeling an SN and an MN using discrete time semi-Markov chain.

For more realistic performance analysis, the relation of node arrival rate, contact time, and inter-contact time was examined with node mobility parameters, such as node velocity, radio transmission range, and node density in the network. Then, the node contact time and inter-contact time are also expressed as PH model. Using this general model the performance of mobile node was analyzed, and then the results were compared with those of Chapter 3. It is examined that the PH model is more closer to the actual distribution than exponential model and the performance by PH model is better than that of exponential model.

Even though our research has dealt with several important issues that have not be considered in the literature there are some subjects that are still not considered in our research. These issues may be considered for further research and are listed as follows:

- DTN can be implemented in various configurations according to its purposes,

and thus to support it, there are diverse routing algorithms. Therefore, in order to establish general power saving framework the algorithm is required to be analyzed in some different routing scenarios.

- To consider the realistic network environment, we need to extend our research to the source nodes which have different characteristics. That is, the mobile source nodes. In this case, the source nodes also need to be equipped with power saving mechanism.

- There are many parameters from node mobility to network configurations that affect the performance of DTN. It is difficult to see the influences of these parameters at the same time. In addition to the numerical evaluations we have provided, simulation is another way to perform dynamic experiments with more intense variation of parameter sets.

Even with limitations, we believe that our work can be helpful by providing some insight on the DTN design.

Appendix

The only non-zero one-step transition probabilities for PH distribution are represented as follows. These probabilities correspond to the one-step transition probabilities for exponential distribution in Chapter 3.

$\mathbf{P_{00}}$: MN stays in SN

$P_{(0,0,k),(0,0,0)} = P\{N(T_k) = 0\}(1 - \boldsymbol{\alpha} e^{\mathbf{T}T_k}\mathbf{1}), \quad k = 0, M+1;$

$P_{(0,0,M+1),(0,0,0)} = P\{N(T_{M+1}) = 0\}(1 - \boldsymbol{\alpha} e^{\mathbf{T}T_{M+1}}\mathbf{1});$

$P_{(0,0,k),(0,j',M+1)} = (1 - P_{col})P\{N(T_k) = j'\}(1 - \boldsymbol{\alpha} e^{\mathbf{T}T_k}\mathbf{1}), \quad 0 \le j' \le K-1, k = 0, M+1;$

$P_{(0,0,k),(0,j',0)} = P_{col}P\{N(T_k) = j'\}(1 - \boldsymbol{\alpha} e^{\mathbf{T}T_k}\mathbf{1}), \quad 0 \le j' \le K-1, k = 0, M+1;$

$P_{(0,0,k),(0,K,M+1)} = (1 - P_{col})\sum_{a=K}^{\infty} P\{N(T_k) = a\}(1 - \boldsymbol{\alpha} e^{\mathbf{T}T_k}\mathbf{1}), \quad k = 0, M+1;$

$P_{(0,0,k),(0,K,0)} = P_{col}\sum_{a=K}^{\infty} P\{N(T_k) = a\}(1 - \boldsymbol{\alpha} e^{\mathbf{T}T_k}\mathbf{1}), \quad k = 0, M+1;$

$P_{(0,j,k),(0,j-1,M+1)} = (1 - P_{col})P\{N(T_k) = 0\}(1 - \boldsymbol{\alpha} e^{\mathbf{T}T_k}\mathbf{1}), \quad k = 0, M+1;$

$P_{(0,j,k),(0,j-1,0)} = P_{col}P\{N(T_k) = 0\}(1 - \boldsymbol{\alpha} e^{\mathbf{T}T_k}\mathbf{1}), \quad k = 0, M+1;$

$P_{(0,j,k),(0,j+l,M+1)} = (1 - P_{col})P\{N(T_k) = l+1\}(1 - \boldsymbol{\alpha} e^{\mathbf{T}T_k}\mathbf{1}), \quad 0 \le l \le K-j-1, k = 0, M+1;$

$P_{(0,j,k),(0,j+l,0)} = P_{col}P\{N(T_k) = l+1\}(1 - \boldsymbol{\alpha} e^{\mathbf{T}T_k}\mathbf{1}), \quad 0 \le l \le K-j-1, k = 0, M+1;$

$P_{(0,j,k),(0,K,M+1)} = (1 - P_{col})\sum_{a=K}^{\infty} P\{N(T_k) = a\}(1 - \boldsymbol{\alpha} e^{\mathbf{T}T_k}\mathbf{1}), \quad k = 0, M+1;$

$P_{(0,j,k),(0,K,0)} = P_{col}\sum_{a=K}^{\infty} P\{N(T_k) = a\}(1 - \boldsymbol{\alpha} e^{\mathbf{T}T_k}\mathbf{1}), \quad k = 0, M+1.$

$\mathbf{P_{02}}$: MN moves from SN to Outside

$P_{(0,0,k),(2,0,0)} = P\{N(T_k) = 0\}\boldsymbol{\alpha}e^{\mathbf{T}T_k}\mathbf{1}, \quad k = 0, M+1;$

$P_{(0,0,k),(2,j',0)} = P\{N(T_k) = j'\}\boldsymbol{\alpha}e^{\mathbf{T}T_k}\mathbf{1}, \quad 0 \le j' \le K-1, k = 0, M+1;$

$P_{(0,0,k),(2,K,0)} = \sum_{a=K}^{\infty} P\{N(T_k) = a\}\boldsymbol{\alpha}e^{\mathbf{T}T_k}\mathbf{1}, \quad k = 0, M+1;$

$P_{(0,j,k),(2,j-1,0)} = P\{N(T_k) = 0\}\boldsymbol{\alpha}e^{\mathbf{T}T_k}\mathbf{1}, \quad k = 0, M+1;$

$P_{(0,j,k),(2,j+l,0)} = P\{N(T_k) = l+1\}\boldsymbol{\alpha}e^{\mathbf{T}T_k}\mathbf{1}, \quad 0 \le l \le K-j-1, k = 0, M+1;$

$P_{(0,j,k),(2,K,0)} = \sum_{a=K}^{\infty} P\{N(T_k) = a\}\boldsymbol{\alpha}e^{\mathbf{T}T_k}\mathbf{1}, k = 0, M+1;$

$\mathbf{P_{11}}$: MN stays in DN

$P_{(1,0,k),(1,0,0)} = P\{N(T_k) = 0\}(1 - \boldsymbol{\beta}e^{\mathbf{S}T_k}\mathbf{1}), \quad k = 0, M+1;$

$P_{(1,0,M+1),(1,0,0)} = P\{N(T_{M+1}) = 0\}(1 - \boldsymbol{\beta}e^{\mathbf{S}T_{M+1}}\mathbf{1});$

$P_{(1,0,k),(1,j',M+1)} = (1 - P_{col})P\{N(T_k) = j'\}(1 - \boldsymbol{\beta}e^{\mathbf{S}T_k}\mathbf{1}), \quad 0 \le j' \le K-1, k = 0, M+1;$

$P_{(1,0,k),(1,j',0)} = P_{col}P\{N(T_k) = j'\}(1 - \boldsymbol{\beta}e^{\mathbf{S}T_k}\mathbf{1}), \quad 0 \le j' \le K-1, k = 0, M+1;$

$P_{(1,0,k),(1,K,M+1)} = (1 - P_{col})\sum_{a=K}^{\infty} P\{N(T_k) = a\}(1 - \boldsymbol{\beta}e^{\mathbf{S}T_k}\mathbf{1}), \quad k = 0, M+1;$

$P_{(1,0,k),(1,K,0)} = P_{col}\sum_{a=K}^{\infty} P\{N(T_k) = a\}(1 - \boldsymbol{\beta}e^{\mathbf{S}T_k}\mathbf{1}), \quad k = 0, M+1;$

$P_{(1,j,k),(1,j-1,M+1)} = (1 - P_{col})P\{N(T_k) = 0\}(1 - \boldsymbol{\beta}e^{\mathbf{S}T_k}\mathbf{1}), \quad k = 0, M+1;$

$P_{(1,j,k),(1,j-1,0)} = P_{col}P\{N(T_k) = 0\}(1 - \boldsymbol{\beta}e^{\mathbf{S}T_k}\mathbf{1}), \quad k = 0, M+1;$

$P_{(1,j,k),(1,j+l,M+1)} = (1-P_{col})P\{N(T_k) = l+1\}(1-\boldsymbol{\beta}e^{\mathbf{S}T_k}\mathbf{1}), \quad 0 \le l \le K-j-1, k = 0, M+1;$

$P_{(1,j,k),(1,j+l,0)} = P_{col}P\{N(T_k) = l+1\}(1 - \boldsymbol{\beta}e^{\mathbf{S}T_k}\mathbf{1}), \quad 0 \le l \le K-j-1, k = 0, M+1;$

$P_{(1,j,k),(1,K,M+1)} = (1 - P_{col})\sum_{a=K}^{\infty} P\{N(T_k) = a\}(1 - \boldsymbol{\beta}e^{\mathbf{S}T_k}\mathbf{1}), \quad k = 0, M+1;$

$P_{(1,j,k),(1,K,0)} = P_{col}\sum_{a=K}^{\infty} P\{N(T_k) = a\}(1 - \boldsymbol{\beta}e^{\mathbf{S}T_k}\mathbf{1}), \quad k = 0, M+1.$

$\mathbf{P_{12}}$: MN moves from DN to Outside

$P_{(1,0,k),(2,0,0)} = P\{N(T_k) = 0\}\boldsymbol{\beta}e^{\mathbf{S}T_k}\mathbf{1}, \quad k = 0, M+1;$

$P_{(1,0,k),(2,j',0)} = P\{N(T_k) = j'\}\boldsymbol{\beta}e^{\mathbf{S}T_k}\mathbf{1}, \quad 0 \le j' \le K-1, k = 0, M+1;$

$P_{(1,0,k),(2,K,0)} = \sum_{a=K}^{\infty} P\{N(T_k) = a\}\boldsymbol{\beta}e^{\mathbf{S}T_k}\mathbf{1}, \quad k = 0, M+1;$

$P_{(1,j,k),(2,j-1,0)} = P\{N(T_k) = 0\}\boldsymbol{\beta}\boldsymbol{\beta}e^{\mathbf{S}T_k}\mathbf{1}, \quad k = 0, M+1;$

$P_{(1,j,k),(2,j+l,0)} = P\{N(T_k) = l+1\}\boldsymbol{\beta}\boldsymbol{\beta}e^{\mathbf{S}T_k}\mathbf{1}, \quad 0 \le l \le K-j-1, k = 0, M+1;$

$P_{(1,j,k),(2,K,0)} = \sum_{a=K}^{\infty} P\{N(T_k) = a\}\boldsymbol{\beta}e^{\mathbf{S}T_k}\mathbf{1}, k = 0, M+1;$

$\mathbf{P_{20}}, \mathbf{P_{21}}$: MN moves from Outside to SN or DN

$P_{(2,0,k),(0/1,0,k+1)} = P\{N(T_k) = 0\}\boldsymbol{\gamma}e^{\mathbf{R}T_k}\mathbf{1}/2, \quad 0 \le k \le M;$

$P_{(2,0,k),(0/1,j',M+1)} = P\{N(T_k) = j'\}\boldsymbol{\gamma}e^{\mathbf{R}T_k}\mathbf{1}/2, \quad 0 \le j' \le K-1, 0 \le k \le M;$

$P_{(2,0,k),(0/1,K,M+1)} = \sum_{a=K}^{\infty} P\{N(T_k) = a\}\boldsymbol{\gamma}e^{\mathbf{R}T_k}\mathbf{1}/2, \quad 0 \le k \le M;$

$P_{(2,j,k),(0/1,j,M+1)} = P\{N(T_k) = 0\}\boldsymbol{\gamma}\boldsymbol{\gamma}e^{\mathbf{R}T_k}\mathbf{1}/2, \quad 0 \le k \le M;$

$P_{(2,j,k),(0/1,j+l+1,M+1)} = P\{N(T_k) = l+1\}\boldsymbol{\gamma}\boldsymbol{\gamma}e^{\mathbf{R}T_k}\mathbf{1}/2, 0 \le l \le K-j-2, 0 \le k \le M;$

$P_{(2,j,k),(0/1,K,M+1)} = \sum_{a=K-1}^{\infty} P\{N(T_k) = a\}\boldsymbol{\gamma}e^{\mathbf{R}T_k}\mathbf{1}/2, \quad 0 \le k \le M.$

$\mathbf{P_{22}}$: MN stays Outside

$P_{(0,0,k),(0,0,k+1)} = P\{N(T_k) = 0\}\boldsymbol{\gamma}(1 - \boldsymbol{\gamma}e^{\mathbf{R}T_k}\mathbf{1}), \quad 0 \le k \le M-1;$

$P_{(0,0,M),(0,0,M)} = P\{N(T_M) = 0\}\boldsymbol{\gamma}(1 - \boldsymbol{\gamma}e^{\mathbf{R}T_M}\mathbf{1});$

$P_{(0,0,k),(0,j',k+1)} = P\{N(T_k) = j'\}\boldsymbol{\gamma}(1 - \boldsymbol{\gamma}e^{\mathbf{R}T_k}\mathbf{1}), \quad 0 \le j' \le K-1, 0 \le k \le M-1;$

$P_{(0,0,M),(0,j',M)} = P\{N(T_M) = j'\}\boldsymbol{\gamma}(1 - \boldsymbol{\gamma}e^{\mathbf{R}T_M}\mathbf{1}), \quad 0 \le j' \le K-1;$

$P_{(0,0,k),(0,K,k+1)} = \sum_{a=K}^{\infty} P\{N(T_k) = a\}\boldsymbol{\gamma}(1 - \boldsymbol{\gamma}e^{\mathbf{R}T_k}\mathbf{1}), \quad 0 \le k \le M-1;$

$P_{(0,0,M),(0,K,M)} = \sum_{a=K}^{\infty} P\{N(T_M) = a\}\boldsymbol{\gamma}(1 - \boldsymbol{\gamma}e^{\mathbf{R}T_M}\mathbf{1});$

$P_{(0,j,k),(0,j,k+1)} = P\{N(T_k) = 0\}\boldsymbol{\gamma}(1 - \boldsymbol{\gamma}e^{\mathbf{R}T_k}\mathbf{1}), \quad 0 \leq k \leq M-1;$

$P_{(0,j,M),(0,j,M)} = P\{N(T_M) = 0\}\boldsymbol{\gamma}(1 - \boldsymbol{\gamma}e^{\mathbf{R}T_M}\mathbf{1});$

$P_{(0,j,k),(0,j+l+1,k+1)} = P\{N(T_k) = l+1\}\boldsymbol{\gamma}(1 - \boldsymbol{\gamma}e^{\mathbf{R}T_k}\mathbf{1}), \quad 0 \leq l \leq K-j-2, 0 \leq k \leq M-1;$

$P_{(0,j,M),(0,j+l+1,M)} = P\{N(T_M) = l+1\}\boldsymbol{\gamma}(1 - \boldsymbol{\gamma}e^{\mathbf{R}T_M}\mathbf{1}), \quad 0 \leq l \leq K-j-2;$

$P_{(0,j,k),(0,K,k+1)} = \sum_{a=K-1}^{\infty} P\{N(T_k) = a\}(1 - \boldsymbol{\gamma}e^{\mathbf{R}T_k}\mathbf{1}), \quad 0 \leq k \leq M-1;$

$P_{(0,j,M),(0,K,M)} = \sum_{a=K-1}^{\infty} P\{N(T_M) = a\}(1 - \boldsymbol{\gamma}e^{\mathbf{R}T_M}\mathbf{1}).$

Bibliography

[1] A. A. Hanbali, R. de Haan, R. J. Boucherie, and J.-K. C. W. van Ommeren, "A tandem queueing model for delay analysis in disconnected ad hoc networks," in *ASMTA'08*, 2008, pp. 189–205.

[2] J. Burgess, B. Gallagher, D. Jensen, and B. Levine, "Maxprop: Routing for vehicle-based disruption-tolerant networks," in *Proc. ieee infocom*, vol. 6. Barcelona, Spain, 2006, pp. 1–11.

[3] P. Juang, H. Oki, Y. Wang, M. Martonosi, L. Peh, and D. Rubenstein, "Energy-efficient computing for wildlife tracking: Design tradeoffs and early experiences with zebranet," in *ACM Sigplan Notices*, vol. 37, no. 10. ACM, 2002, pp. 96–107.

[4] E. Brewer, M. Demmer, B. Du, M. Ho, M. Kam, S. Nedevschi, J. Pal, R. Patra, S. Surana, and K. Fall, "The case for technology in developing regions," *Computer*, vol. 38, no. 6, pp. 25–38, 2005.

[5] S. Burleigh, A. Hooke, L. Torgerson, K. Fall, V. Cerf, B. Durst, K. Scott, and H. Weiss, "Delay-tolerant networking: an approach to interplanetary internet," *Communications Magazine, IEEE*, vol. 41, no. 6, pp. 128–136, 2003.

[6] S. Jain, R. Shah, W. Brunette, G. Borriello, and S. Roy, "Exploiting mobility for energy efficient data collection in wireless sensor networks," *Mobile Networks and Applications*, vol. 11, no. 3, pp. 327–339, 2006.

[7] W. Zhao and M. Ammar, "Message ferrying: Proactive routing in highly-partitioned wireless ad hoc networks," in *Distributed Computing Systems, 2003. FTDCS 2003. Proceedings. The Ninth IEEE Workshop on Future Trends of*. IEEE, 2003, pp. 308–314.

[8] A. Vahdat and D. Becker, "Epidemic routing for partially connected ad hoc networks," 2000.

[9] J. Davis, A. Fagg, and B. Levine, "Wearable computers as packet transport mechanisms in highly-partitioned ad-hoc networks," in *Wearable Computers, 2001. Proceedings. Fifth International Symposium on*. IEEE, 2001, pp. 141–148.

[10] T. Small and Z. Haas, "The shared wireless infostation model: a new ad hoc networking paradigm (or where there is a whale, there is a way)," in *Proceedings of the 4th ACM international symposium on Mobile ad hoc networking & computing*. ACM, 2003, pp. 233–244.

[11] R. Groenevelt, P. Nain, and G. Koole, "The message delay in mobile ad hoc networks," *Performance Evaluation*, vol. 62, no. 1, pp. 210–228, 2005.

[12] A. Chaintreau, P. Hui, J. Crowcroft, C. Diot, R. Gass, and J. Scott, "Impact of human mobility on opportunistic forwarding algorithms," vol. 6, no. 6. IEEE, 2007, pp. 606–620.

[13] T. Spyropoulos, K. Psounis, and C. Raghavendra, "Performance analysis of mobility-assisted routing," in *Proc. of the 7th ACM international symposium on Mobile ad hoc networking and computing*. ACM, 2006, p. 60.

[14] C. Chiasserini and R. Rao, "A distributed power management policy for wireless ad hoc networks," in *Wireless Communications and Networking Conference, 2000. WCNC. 2000 IEEE*, vol. 3. IEEE, 2000, pp. 1209–1213.

[15] B. Chen, K. Jamieson, H. Balakrishnan, and R. Morris, "Span: An energy-efficient coordination algorithm for topology maintenance in ad hoc wireless networks," *Wireless Networks*, vol. 8, no. 5, pp. 481–494, 2002.

[16] W. Ye, J. Heidemann, and D. Estrin, "An energy-efficient mac protocol for wireless sensor networks," in *INFOCOM 2002. Twenty-First Annual Joint Conference of the IEEE Computer and Communications Societies. Proceedings. IEEE*, vol. 3. IEEE, 2002, pp. 1567–1576.

[17] T. Van Dam and K. Langendoen, "An adaptive energy-efficient mac protocol for wireless sensor networks," in *Proceedings of the 1st international conference on Embedded networked sensor systems*. ACM, 2003, pp. 171–180.

[18] V. Rajendran, K. Obraczka, and J. Garcia-Luna-Aceves, "Energy-efficient, collision-free medium access control for wireless sensor networks," *Wireless Networks*, vol. 12, no. 1, pp. 63–78, 2006.

[19] *IEEE Std 802.16e-2005: IEEE Standard for Local and metropolitan area networks Part 16: Air Interface for Fixed and Mobile Broadband Wireless Access Systems Amendment 2: Physical and Medium Access Control Layers for*

Combined Fixed and Mobile Operation in Licensed Bands and Corrigendum 1, Std., February, 2006.

[20] M. Kim, M. Kang, and J. Choi, "Remaining energy-aware power management mechanism in the 802.16 e mac," in *Consumer Communications and Networking Conference, 2008. CCNC 2008. 5th IEEE.* IEEE, 2008, pp. 222–226.

[21] O. Vatsa, M. Raj, K. Ritesh Kumar, D. Panigrahy, and D. Das, "Adaptive power saving algorithm for mobile subscriber station in 802.16 e," in *Communication Systems Software and Middleware, 2007. COMSWARE 2007. 2nd International Conference on.* IEEE, 2007, pp. 1–7.

[22] F. Xu, W. Zhong, and Z. Zhou, "A novel adaptive energy saving mode in ieee 802.16 e system," in *Military Communications Conference, 2006. MILCOM 2006. IEEE.* IEEE, 2006, pp. 1–6.

[23] H. Jun, M. Ammar, and E. Zegura, "Power management in delay tolerant networks: A framework and knowledge-based mechanisms," in *IEEE Communications Society Conference on Sensor and Ad Hoc Communications and Networks (SECON).* Citeseer, 2005.

[24] H. Guo, J. Li, A. Washington, C. Liu, M. Alfred, R. Goel, L. Burge, and P. Keiller, "Performance analysis of homing pigeon based delay tolerant networks," in *Military Communications Conference, 2007. MILCOM 2007. IEEE.* IEEE, 2007, pp. 1–7.

[25] D. Niyato, P. Wang, and J. Teo, "Performance analysis of the vehicular delay tolerant network," in *Wireless Communications and Networking Conference, 2009. WCNC 2009. IEEE.* IEEE, 2009, pp. 1–5.

[26] Y. Wang, H. Wu, and H. Dang, "Analytic study of delay/fault-tolerant mobile sensor networks (dft-msn's)," in *World of Wireless, Mobile and Multimedia Networks & Workshops, 2009. WoWMoM 2009. IEEE International Symposium on a.* IEEE, 2009, pp. 1–9.

[27] H. Shen, L. Cai, and X. Shen, "Performance analysis of TFRC over wireless link with truncated link-level ARQ," *IEEE Transactions on Wireless Communications*, vol. 5, no. 6, p. 1479, 2006.

[28] S. Pack, X. Shen, J. Mark, and L. Cai, "A two-phase loss differentiation algorithm for improving tfrc performance in ieee 802.11 wlans," *IEEE Transactions on Wireless Communications*, vol. 6, no. 11, p. 4164, 2007.

[29] F. Eshghi and A. Elhakeem, "Performance analysis of ad hoc wireless LANs for real-time traffic," *IEEE Journal on Selected areas in communications*, vol. 21, no. 2, pp. 204–215, 2003.

[30] J. Broch, D. Maltz, D. Johnson, Y. Hu, and J. Jetcheva, "A performance comparison of multi-hop wireless ad hoc network routing protocols," in *Proc. of the 4th annual ACM/IEEE international conference on Mobile computing and networking.* ACM New York, NY, USA, 1998, pp. 85–97.

[31] P. Johansson, T. Larsson, N. Hedman, B. Mielczarek, and M. Degermark, "Routing protocols for mobile ad-hoc networks-a comparative performance

analysis," in *Proc. of the 5th International Conference on Mobile Computing and Networking (ACM MOBICOM)*, 1999, pp. 195–206.

[32] S. Das, C. Perkins, E. Royer, and M. Marina, "Performance comparison of two on-demand routing protocols for ad hoc networks," in *Proc. of IEEE INFOCOM*, vol. 1. Citeseer, 2000, pp. 3–12.

[33] C. Bettstetter, "Mobility modeling in wireless networks: categorization, smooth movement, and border effects," *ACM SIGMOBILE Mobile Computing and Communications Review*, vol. 5, no. 3, pp. 55–66, 2001.

[34] K. Wang and B. Li, "Group mobility and partition prediction in wireless ad-hoc networks," in *IEEE International Conference on Communications*, vol. 2. Citeseer, 2002, pp. 1017–1021.

[35] E. Tan, S. McLaughlin, and D. Laurenson, "An analytical model for differentiated services in wireless mobile ad-hoc network," in *2004 IEEE 60th Vehicular Technology Conference, 2004. VTC2004-Fall*, vol. 4, 2004.

[36] Y. Dong and D. Makrakis, "Network Congestion Control and QoS Support on Mobile Wireless Multihop Ad-Hoc Networks," in *Proc. of the 6th Wireless Personal Multimedia Communications (WPMC)*, October 2003, pp. 314–319.

[37] B. Kwak, N. Song, and L. Miller, "A mobility measure for mobile ad hoc networks," *IEEE Communications Letters*, vol. 7, no. 8, pp. 379–381, 2003.

[38] M. Abdulla and R. Simon, "Characteristics of common mobility models for opportunistic networks," in *Proc. of the 2nd ACM workshop on Performance monitoring and measurement of heterogeneous wireless and wired networks (PM2HW2N)*, 2007, pp. 105–109.

[39] T. Small and Z. Haas, "Resource and performance tradeoffs in delay-tolerant wireless networks," in *Proc. of the 2005 ACM SIGCOMM workshop on Delay-tolerant networking*. ACM, 2005, p. 267.

[40] N. Sadagopan, F. Bai, B. Krishnamachari, and A. Helmy, "PATHS: analysis of PATH duration statistics and their impact on reactive MANET routing protocols," in *Proc. of the 4th ACM international symposium on Mobile ad hoc networking & computing*. ACM New York, NY, USA, 2003, pp. 245–256.

[41] Y. Han, R. La, A. Makowski, and S. Lee, "Distribution of path durations in mobile ad-hoc networks - Palm's Theorem to the rescue," *Computer Networks*, vol. 50, no. 12, pp. 1887–1900, 2006.

[42] G. Latouche, V. Ramaswami, and V. Kulkarni, *Introduction to matrix analytic methods in stochastic modeling*. NORTH ATLANTIC SCIENCE PUBLISHING COMPANY, 1999, vol. 12, no. 4.

[43] P. Samar and S. Wicker, "On the behavior of communication links of a node in a multi-hop mobile environment," in *Proc. of the 5th ACM international symposium on Mobile ad hoc networking and computing (MobiHoc)*, June 2004, pp. 145–156.

[44] S. Cho and J. Hayes, "Impact of mobility on connection in ad hoc networks," in *Proc. of IEEE Wireless Communications and Networking Conference*, New Orleans, March 2005, pp. 1650–1656.

[45] D. Johnson and D. Maltz, "Dynamic source routing in ad hoc wireless networks," *KLUWER INTERNATIONAL SERIES IN ENGINEERING AND COMPUTER SCIENCE*, pp. 153–179, 1996.

[46] C. Bettstetter, G. Resta, and P. Santi, "The node distribution of the random waypoint mobility model for wireless ad hoc networks," *IEEE Transactions on Mobile Computing*, vol. 2, no. 3, pp. 257–269, 2003.

[47] J. Yoon, M. Liu, and B. Noble, "Random waypoint considered harmful," in *Proc. of IEEE INFOCOM*, San Francisco, April 2003, pp. 1312–1321.

[48] A. Alfa, "Queueing theory for telecommunications," *Queueing Theory for Telecommunications: Discrete Time Modelling of a Single Node System, ISBN 978-1-4419-7313-9. Springer Science+ Business Media, LLC, 2010*, vol. 1, 2010.

[49] S. Leng, L. Zhang, H. Fu, and J. Yang, "Mobility analysis of mobile hosts with random walking in ad hoc networks," *Computer Networks*, vol. 51, no. 10, pp. 2514–2528, 2007.

[50] S. Asmussen, O. Nerman, and M. Olsson, "Fitting phase-type distributions via the em algorithm," *Scandinavian Journal of Statistics*, pp. 419–441, 1996.